Synthesis and Characterization of BST Ceramics by Solution Combustion Technique

A Thesis Submitted in Partial Fulfillment of the Requirements
for the Degree of

Bachelor of Technology

by

Suraj Kumar Das (Roll No. 107CR027)

Department of Ceramic Engineering.
National Institute of Technology,
Rourkela, Odisha.

Synthesis and Characterization of BST Ceramics by Solution Combustion Technique

A Thesis Submitted in Partial Fulfillment of the Requirements for the Degree of

Bachelor of Technology

by

Suraj Kumar Das (Roll No. 107CR027)

Supervisor:

Dr. Swadeh Kumar Pratihar

Department of Ceramic Engineering.
National Institute of Technology,
Rourkela, Odisha.

ACKNOWLEDGEMENTS

With deep regards and profound respect, I avail this opportunity to express my deep sense of gratitude and indebtedness to Dr. Swadesh Kumar Pratihar, Department of Ceramic Engineering, N. I. T. Rourkela, for introducing the present research topic and for inspiring guidance, constructive criticism and valuable suggestion throughout this research work. It would have not been possible for me to bring out this project report without his help and constant encouragement. I wish that he will keep in touch with me in future and will continue to give his valuable advice.

I would like to express my gratitude, to all the faculties of Department of Ceramic Engineering, whose vast knowledge in the field of science and technology has enlightened me in different areas of this experimental research work. I am also thankful to Miss. Gitanjali Parida and Mr Sarat Kumar Rout for helping me in the lab.

I would also like to thank my friends, especially Debesh Daulat Mohanty and Sourav Pattanik for helping me in the completion of this project work.

Above all, I thank GOD for giving me the encouragement, skills and opportunity to complete this report.

Date: (Suraj Kumar Das)

National Institute of Technology Rourkela

CERTIFICATE

This is to certify that the thesis entitled, *"Synthesis and Characterization of BST Ceramics by Solution Combustion Technique"* submitted by Mr. **Suraj Kumar Das** in partial fulfillments for the requirements for the award of **Bachelor of Technology** degree in **Ceramic Engineering** at National Institute of Technology, Rourkela is an authentic work carried out by him under my supervision and guidance.

To the best of my knowledge, the matter embodied in the thesis has not been submitted to any other University/ Institute for the award of any Degree or Diploma.

Date:

Dr. Swadesh Kumar Pratihar
Dept. of Ceramic Engineering
National Institute of Technology
Rourkela-769008

Contents

Lists of Figures

Lists of Tables

Abstract

Abstract

Barium Strontium Titanate ($Ba_{0.6}Sr_{0.4}TiO_3$) has been prepared and characterized in this present study. Phase pure BST powder has been prepared following combustion synthesis technique. Citric acid, ethylene glycol and glycine have been used as a fuel in this combustion process. Different process parameters mainly additional NH_4NO_3, citric acid as fuel amount, additional chelating agent EDTA and pH of the precursor solution has been optimized with an aim to achieve phase pure BST at a low temperature. Effect of mixed fuel i.e. citric acid + ethylene glycol and citric acid + glycine, has also been studied as a function of powder morphology of BST powder. The optimum precursor combination Metal: Citric Acid: Ammonium Nitrate: EDTA are: 1:1.5:12:0.1 at pH of the precursor solution 7, has been found to yield phase pure BST powder at 800^oC. The densification behavior and densification kinetics of the BST powder has also been studied. Powder morphology and microstructure of sintered BST samples was found to depend strongly on the fuel used for combustion. Dielectric behavior of BST samples has also been studied as a function of fuel used.

Chapter 1

Introduction

Introduction:

Barium Strontium Titanate(BST) is mainly used in piezoelectric sensors, dynamic random access memory (DRAM), microwave phase shifters and infrared detectors. BST with its high dielectric, ferroelectric, pyroelectric properties and as a lead free material has generated greater interest.[1].BST has attracted attention due to its strong dielectric nonlinearity under bias electric field and linearly adjustable Curie temperature with the strontium content over a wide temperature range

With rapid advancements in the field of communication, there has been an ever increasing demand for very powerful and low cost microwave systems for the use in fast band switching in multimedia services. It is being widely used because of the high data transmitting rates which is a requirement in fast data transfer.

They are also used in electronically steerable antennas in automobiles which serve the purpose of safe navigation of vehicle in case of any difficulty. As a part of collision radars, they have helped to improve the safety of people. Tunable microwave components like varactors, filters, oscillators and phase shifters currently based on PIN diodes, GaAs Schottky diodes or ferromagnetics help to achieve tunability and band switching.[2]

But in contrast to these microwave components, the ferroelectric components have a distinct advantage over them. They provide continuous, quick and low power tenability up to very high frequencies. The tunability of ferroelectric materials is based on the nonlinear behavior of internal electrical polarization with the external electromagnetic field of the steerable radars. There is also marked cost reduction due to integration in the ferroelectric ceramic materials. This has renewed interests for research in BST material systems to be used in room temperature.

The tunablity of BST makes it a perfect candidate for microwave applications. The uses of BST in tunable microwave devices have been explored in various forms, such as bulk ceramics, thin films and thick films. BST thin films has a disadvantage of higher production cost, hence powder production is still one of the important aspect of research.

BST is also used as composite with $La_{0.7}Ca_{0.3}MnO_3$ [3], $BaZn_6Ti_6O_{19}$ [4], MgO [5], $ZnNb_2O_6$ [6] and Mn [7] to either increase its efficiency or to diversify its application area.

The property of the BST depends on factors like grain size, grain morphology, sintering temperature, sintering conditions, doping amount, porosity, and structural defects. Hence property of the BST can also be tailored by controlling the above parameters.

BST powders have been prepared by different process and each process has its own merits and demerits. Sol gel method is costly, time consuming and its precursors are sensitive to moisture, temperature and even light [8][9]. Co-Precipitation requires repeated washing of the precipitate to remove the soluble anions from the precipitate making the process time consuming and complicated [10][11]. In mechanochemical synthesis high energy is consumed for milling and particle homogeneity is also not maintained and also there is a chance of contamination.

Combustion synthesis is a very important technique for the synthesis of very high purity nano materials [12][13]. Advantages of combustion synthesis over the above mentioned process is that its cost effective, produces uniform particle size, energy efficient less probability of contamination and high production rate.

The property of the powder formed depends on a lot of factors which govern the kinetics of the combustion reaction which are called process parameters. In the literature we don't find any optimization for these parameters. For example we know that NH_4NO_3 addition enhances the

productivity of the powders but we don't know in what ration NH_4NO_3 must be added for better results.

Fuels used in the combustion precursor also have significant effect on the properties of the powder. Though combustion is mainly carried out using citric acid but a large number of other fuels are also available like glycine, ethylene glycol, urea, tartaric acid etc. One of the main problems with these fuels is that they do not provide chelating action like citric acid; hence mostly these fuels are used in combination with other chelating agents like EDTA or citric acid.

Chapter 2

Literature Review

2. Literature Review

Since the development of BST several aspects pertaining to its property has been studied. In the recent years, the work is mainly focused on the tailoring the morphology of the powder and particle size, thin film fabrication and improvement of the tenability of the ceramics.

Liu et al. [14] have synthesized $Ba_{0.5}Sr_{0.5}TiO_3$ powders using citrate–nitrate combustion technique. The precursor used was barium nitrate, strontium nitrate, tetrabutyl titanate and ammonia. It has been reported that phase pure BST could be obtained at temperatures above 700^{o}C. The BST powder synthesized in this technique was very fine about 40 nm. Samples sintered by spark plasma sintering showed improved dielectric

Longxiang et al. [15] have synthesized uninodal and narrow particle size cuboidal BST nanoparticles in a glycothermal route using oleic acid in form of a growth directing agent. Effect of different process parameters like oleic acid amount, duration of reaction and 1,4-butanediol/water volume ratio on phase purity, particle morphology and distribution. They found that presence of oleic acid in the glycothermal system promotes the yield of nanocrystals. The BST nanocrystals are formed through seeding and growth process. Oleic acid adsorption on facets having lower value of plane indices of the BST nuclei directs the growth forming cuboidal BST nanocrystals. The resultant BST particles are self-assembling in nature in organic solvents. They are dropped on hydrophobic substrate's surface, causing the nano-crystals to self-assemble forming nano electronic devices.

BST powder was synthesized with M:CA ration keeping 1:1.5, and addition of NH_4NO_3 as a combustion promoter. [16]. DTA of the gel revealed that a large exothermic peak at about 450°C occurred with about 38% weight loss. Addition of NH_4NO_3 favors the reaction and gives a more uniform particle size distribution, and those without it are non-uniform and agglomerated in

nature. The NH_4NO_3 produced huge amount of gasses which made the powder fluffy and soft in nature.

Haixin et al, synthesized BST nano particles by hydrolysis method using N,N-dimethylacetamide as a solvent at 120 °C and 140 °C[9]. The as-prepared particles presented a perovskite polycrystalline structure. The particle sizes were in the range of 5 – 30 nm. Good dielectric properties were displayed by the composition without any annealing treatment characterized with the parallel plate capacitor method. The thermal reaction of barium acetate, strontium acetate and tetrabutyltitanate in N,N-dimethylacetamide helped to synthesize ferroelectric nanoparticles of BST. The temperature for synthesis can greatly affect the crystallinity of the sample. The dielectric loss varied from 1.1% to 3.7%. The dielectric constant decreased to a small valueabruptly with the increase of frequency. When curves of dielectric loss as a function of frequency were studied a maximum dielectric loss was observed. Restriction of mobile charges in BST ceramics by the reduced relaxation effect under a high frequency can be a possible reason for this observation.

Leiqing et al, synthesized BST spherical nano particles having size 20-80 nm in a microwave-activated glycothermal route [17]. Effect of different process conditions like the microwave irradiation duration, 1,4-butanediol/water and Ba/(Ba + Sr) on composition, particle-sizes and morphologies were studied. It was reported that BST crystals formed within 1 min in the microwave-glycothermal process through an in situ reaction kinetics, where the highly dispersed $TiO_2 \cdot xH_2O$ colloidal particles which are amorphous in nature reacts with Ba^{2+} and Sr^{2+} ions and then coarsening occurs. The particle size, morphology, composition and crystal structure of BST particles can be tailored by influencing the process parameters

The solvothermal synthesis of single-crystalline BST nanocubes was done using $TiCl_4$–$BaCl_2$ as precursors in the mixed solvent of water–ethanol–ethylene glycol monomethylether [18]. Being of regular cubic shape, the as-prepared BST powder with cubic perovskite structure is important in the study of the relationship of particle shape and material performance. BST nanocubes are well dispersed with narrow particle size distribution and thus are attained by this simple solvothermal method. The Sr/(Sr + Ba) mole ratio in reactants determines the particle morphology and size of powders.The crystal size of BST increases slightly in comparison with pure $BaTiO_3$ nanocube prepared by the solvothermal method, with however, the particle size decreases as expected.

A modified oxalate co-precipitation method was used to obtain Single-phase BSTO powders i.e. the quantitative barium–strontium titanyl oxalate (BSTO) precursor powders [11]. The principle behind it finds its basis in the cation-exchange reaction between the stoichiometric solutions of oxalotitanic acid (HTO) and barium + strontium nitrate solution containing stoichiometric quantities of Ba and Sr ions. On pyrolysis of the aforementioned BSTO at 800°C/4 h in air homogeneous cauliflower-like morphology of BST powders is produced. Concrete investigation was carried out on the effect of polyethylene glycol (PEG) on morphology of BSTO and BST powders. The BSTO and BST powders yielded in the following technique without PEG, displayed homogeneity with noticeable spherical shape. On the effect of PEG, the powders grew into spindle shape.

A wet chemical synthesis technique for large-scale fabrication of perovskite BST nano-particles near room temperature and under ambient pressure is reported in the process which employs titanium alkoxide and alkali earth hydroxides as starting materials and involves very simple operation steps [19]. By changing the processing parameters, particle size and crystallinity of the

particles are controlled. The particles were well-crystallized, chemically stoichiometric and 50 nm in diameter. The nanoparticles show typical ferroelectric hysteresis loops and can be sintered into ceramics at 1150°C. .

Khemprasit et al, fabricated BST nanofibers by electro-spinning method using a solution that contained poly(vinylpyrrolidone) and a sol–gel solution of BST is studied[20] .Calcinations of the as-spun BST/PVP composite nano fibers at above 700°C in air for 2 h, helps to obtain BST nano fibers of 188±25 nm in diameter having well-developed cubic-perovskite successfully. The crystal structure and morphology of the nano fibers were influenced by the calcination temperature. Calcination at below 700°C resulted in amorphous phase whereas BST with second phase such as barium titanate were formed at above 700°C. Diameters of the nano fibers decreased from 208±35 to 161±18 nm with increasing calcination temperature between 600 and 800°C.Thenanofibers consisted of the structure of packed particles or crystallites of 40–60 nm. The electrospun BST nano fibers could have potential in some new applications as ferroelectric BST fibers for nano composites and as electronic material for nano devices and is has generated interests among the researchers.

Berbecaru, [21] synthesized $Ba_{0.6}Sr_{0.4}TiO_3$ (BST 40) by solid-state reaction at 1210-1450°C. Densification of 94% was attained. Normal as well as abnormal grain growth was observed in the microstructure. Presence of secondary phase was also there. Dielectric behavior was studied in the range of - 150°C to + 150°C, and 150 Hz-5 MHz. It was reported that with increasing sintering temperature permittivity value increased. Sharp and well defined transition peaks were reported for high temperature of sintering. Low values of permittivity were obtained for microwave measurements at room temperature. Dielectric losses were reported to be less than

1% at 0.7 GHz. The sintering schedule and phase purity of precursor materials results in changed transition temperature for varying Sr content which was sintered at 1260°C for 2 h.

Longo et al, [22] synthesized BST in the temperature range 100-130 °C through Hydrothermal-microwave method (HTMW). $BaCO_3$ as impurity was present at lower temperature of synthesis. Lattice OH- groups, were found in the synthesized sample. Particles were of the range of 40-80 nm. Lower sintering temperature yield small and uniform grains while at high temperature there are large grains embedded in a matrix of small grains. HTMW route was reported to be rapid, cost effective, and an alternative route to obtain BST nanoparticles.

Mansingh et al, synthesized BST thin films in the sol–gel technique on platinized silicon substrate for the composition range x = 0.0 to 1.0 in steps of 0.1 [23]. The as-deposited films which were amorphous initially, crystallized on annealing in air at 700°C for 1 h. In the temperature range − 180°C to 150°C and in the frequency range 0.1 to 100 kHz dielectric constant (ε′) and loss tangent (tanδ) were measured. A small dispersion for all the compositions is shown for both ε′ and tanδ this is more at the peak value than at room temperature. Except strontium titanate all the compositions show a transition from ferroelectric to paraelectric phase and also the transition temperature shows a systematic decrease with increase in strontium content. The variation is found at a rate of 3.4°C/mol% of $SrTiO_3$. The room temperature dielectric constant variation with barium content shows maxima at the compositions x = 0.4 and x = 0.8. The dielectric constant and dielectric loss for all the compositions show very little frequency dispersion in the range 0.1 to 100 kHz for films deposited on platinized silicon substrate. This may be attributed to the contribution from the hopping conduction and to the dispersion due to the barrier layer at the film electrode interface and at the grain boundaries. A diffuse phase transition for all the frequencies is shown by the various compositions used and the

diffusivity increases with increasing Sr content. Near about the bulk transition temperature, all the compositions except x = 0.0 show a transition from ferroelectric to paraelectric phase.

Chapter 3

Objective of Work

3. Objective:

In the present work we will be synthesizing BST powders through solution combustion route. The following work has been covered:

1. Optimization of the process parameters in the citrate-nitrate route
2. Sintering behavior of the powder produced.
3. Microstructure of the sintered powder as a function of sintering temperature
4. Study of dielectric behavior of the sintered sample
5. Correlation between the above produced powder with the samples produced by a mixture of CA + Glycine and CA+ Ethylene Glycol

Chapter 4

Experimental Procedure

4. Experimental Procedure:

BST powders were synthesized using the combustion synthesis technique. Combustion synthesis is a relatively new method for synthesizing phase pure multi-component single phase material having a uninodal particle size distribution. Combustion synthesis is mainly a reaction between the metal complexes formed with the fuel or chelating agents and the oxidant. In this method, the precursor materials, which are preferably nitrates salts of the metal, are made soluble in water. Then a fuel and/or chelating agent is added to this solution and then the desired pH is achieved. The oxidant is mainly the nitrate ion that's being derived from the metal salt or the presence of nitrate ion present in the solution or, in some cases, additional ammonium nitrate is added as an oxidant material. The fuels that had been used in this work are citric acid, glycine and ethylene glycol, and the additional chelating agent used was EDTA.

The above precursor solution containing the metal nitrates forms a soluble complexes with the fuels and/or the chelating agents which on further heating at 80°C-90°C forms a viscous gel. The gel thus formed undergoes dehydration on further heating and self-ignites with the evolution of huge amount of gases. Hence the residual ash that is formed after combustion has a floppy structure. This ash is further calcined to get the pure phase powder. The complex formation and self-ignition or decomposition of the gel depends on a number of process parameters.

In the present study, $Ba_{0.6}Sr_{0.4}TiO_3$, powder was prepared using combustion synthesis technique. The precursors for the metal cation were $TiO(NO_3)_2$, $Ba(NO_3)_2$ and $Sr(NO_3)_2$. The $TiO(NO_3)_2$ was prepared in house. The fuel used wascitric acid for optimizing the process parameters, and then a mixture of citric acid and glycine and a mixture of citric acid and ethylene glycol. The other constituents were EDTA as chelating agent and ammonium nitrate as an additional oxidant.

The different experimental techniques used in the present study have been discussed below.

4.1 Preparation of $TiO(NO_3)_2$:

TiO_2 is only soluble in sulphuric acid (H_2SO_4) and forms titanium oxy-sulphate ($TiO(SO_4)$). The rate of formation of $TiO(SO_4)$ is enhanced in the presence of ammonium sulphate ($(NH_4)_2SO_4$). The reaction kinetics got enhanced on maintaining a temperature of 90°C-95°C. The procedure for $TiO(NO_3)_2$ solution preparation is discussed below.

First $(NH_4)_2SO_4$ {Merck}, was added into concentrated H_2SO_4{Merck} and was stirred till it dissolved. Weighted amount of TiO_2 {Merck} was then added to this solution and stirred. TiO_2, $(NH_4)_2SO_4$ and H_2SO_4 was in the ration of 1gm:6gm:12ml. After adding TiO_2 it forms a suspension which needs to be vigorously stirred over a hot plate until the suspension turns into a clear solution. The reaction that occurs can be written as:

$$TiO_2 + H_2SO_4 \text{—>} TiO(SO_4) + H_2O$$

This solution was cooled for 12 hours and then diluted with water in the ratio of 1:2, and titrated against ammonium hydroxide (NH_4OH) {Oster} solution, which gives rise to a white precipitate. The reaction that occurs can be written as:

$$TiO(SO_4) + 2NH_4OH \text{—>} TiO(OH)_2 \downarrow + (NH_4)_2SO_4$$

The precipitate was washed until it gets sulphate free. Then this precipitate was dissolved in a 1:1 dilute nitric acid (HNO3) {Merck}. The reaction that occurs can be written as:

$$TiO(OH)_2 + 2HNO_3 = TiO(NO_3)_2 + 2H_2O$$

The strength of the Ti^{+4} present in the solution was determined by gravimetric technique.

4.2 Combustion Synthesis of BST powders:

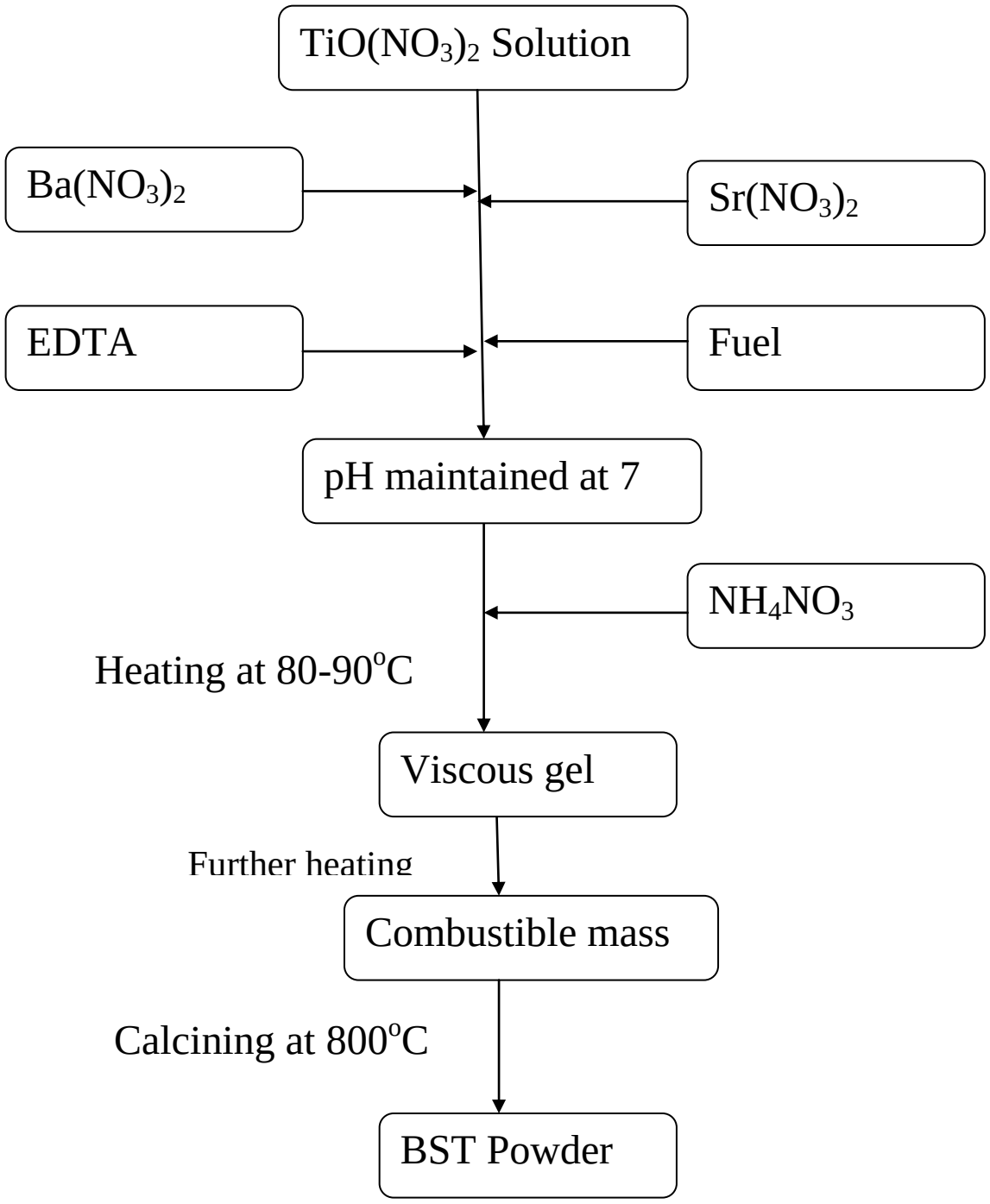

Fig 4.1 Flow chat for the powder production

BST powder was prepared using citrate-nitrate combustion synthesis method. Precursors used for synthesis were $TiO(NO_3)_2$ {as prepared}, $Ba(NO_3)_2$ {LobaChemie}, citric acid {Merck}(and glycine{Qualigens} or ethylene glycol{Qualigens}), ammonium nitrate NH4NO3 {Merck}and Ethylene diamine tetra acetic acid(EDTA) {LobaChemie}. Required amount of above precursors were taken together. pH of the solution was adjusted using NH_4OH.The solution was placed on the hot plate. The temperature of the hot plate was kept in the range of 80°C-90°C Dehydration of the homogeneously mixed solution forms a viscous gel. This gel on further heating swells and then self-ignites. The ash that was produced was voluminous and floppy in nature. This ash on calcination yield phase pure BST powder. The calcinations were done at 800°C and the rate of heating was 3°C/min. The flow chart for the powder synthesis is given in Fig. 4.1

4.3Powder Characterization:

4.3.1. Thermal Decomposition behavior of the Gel:

Thermal decomposition behavior of the gel has been studied using Netzsch, STA 449C. The DSC/TG patterns were collected as a function of temperature and time up to 900°C under N_2 atmosphere. The heating rate was 10°C/min. Reference material used was alpha alumina.

4.3.2 Phase Analysis

The calcined powder sample and the sintered samples were analyzed for the phase present using the X-Ray diffraction technique (Philips PAN analytical, The Netherland) using CuK_α radiation. The generator voltage was 35 KV and current was 25 mA.Phases present were analyzed by the Philips X'pertHighscore software.

4.4. Preparation of bulk sample:

Calcined powder was mixed with 3 wt.% PVA (Poly Vinyl Alcohol) binder. The binder mixed powder was dried and was compacted to give a desired shape for further characterization. The

binder mixed powders were pressed uniaxially in a HC-HCr die intocylindrical pellets (12 mmΦ). The uniaxial pressing was done at 4T pressure in a hydraulic press (10 T, Carver Industries, USA). A holding time of 120seconds was givenfor pressing of each sample. The pressed green compacts were sintered in air with a heating rateof 3°C/min at the temperature ranges 1250°C -1350°C with a holding time of 4 hours in electrical furnace. The bulk density and apparent porosity of the sintered specimen were measured byArchimedes Principle.

4.5. Densification Study:

The densification behavior and sintering kinetics have been studied using NETZSCH DL 420 Dilatometer in the isothermal as well as non-isothermal (Constant Rate Heating) conditions.

4.6. Microstructural Analysis:

Microstructure of calcined powders and sintered pellets has been studied using Scanning Electron Microscope (JOEL-JSM 6480LV). The generator voltage was 15kV. The powder samples were dispersed in isopropyl alcohol and deposited on glass slides. The sintered pellets were washed in isopropyl alcohol. The samples were electroplated with platinum for making the surface conducting.

4.7. Dielectric Measurement:

The sintered pellets were polished and coated with silver paste [Alkem]. Then they were cured at a temperature of 600°C for 1hr. Dielectric Measurement of the samples have been done using the Solatron S1 1260 Impedance/Grain-phase analyser with Solatron 1296 dielectric interface. The frequency range for the dielectric measurement was varied from 1Hz to 1MHz. The dielectric measurement was also studied as a function of temperature. The temperature was varied from 40°C to 150°C.

Chapter 5

Results and Discussion

5. Results and Discussions:

5.1 Optimization of Process Parameters using Citric Acid as Fuel:

Combustion synthesis is an important technique for the synthesis of pure phase ceramic materials. The exothermicity of the redox reaction between the fuel and the oxidant is utilized to form the powder. BST is synthesized using this technique. The property of the powder formed depends on a several factors which govern the kinetics of the combustion reaction are called process parameters.

These process parameters include citric acid (CA), ammonium nitrate (O) as oxidant, ethylenediaminetetra-acetic acid (EDTA) and pH of the solution. In this optimization process attempt has been made to first optimize a single component and then keeping that constant optimize the next component. All the optimizations were done by analyzing the DSC plots of the gel and XRD plots of the calcined powders.

5.1.1 Optimization of Ammonium Nitrate:

A through literature review show that the better BST powder could be prepared while CA molar amount was taken to be 1.5 with respect to the metal ion concentration[10]; the pH was of the precursor solution should be in the range 6-7 [9], and the ammonium nitrate was a preferred combustion promoter [10]. In this work some amount of EDTA has also been added as an extra chelating agent.

Hence the initial molar ratio of Metal (M):CA:EDTA=1:1.5:0.1, the pH =7 and the molar amount of NH_4NO_3 was varied as 4, 8 and 12.The DSC of the gel as a function of different NH_4NO_3 concentration is in the Fig. 5.1 and the XRD of the calcined powders calcined at 800°C were

shown as a function of different NH_4NO_3 concentration in the Fig. 5.2; Table I, shows the different molar ratios in the different batches used for optimizing the NH_4NO_3.

TableI. Molar ratio of different process parameters in different batches for the optimization of NH_4NO_3

Metal(M)	Citric Acid(CA)	NH_4NO_3 (O)	EDTA	pH	Phase Purity
1	1.5	4	0.1	7	Impure
1	1.5	8	0.1	7	Impure
1	1.5	12	0.1	7	Pure

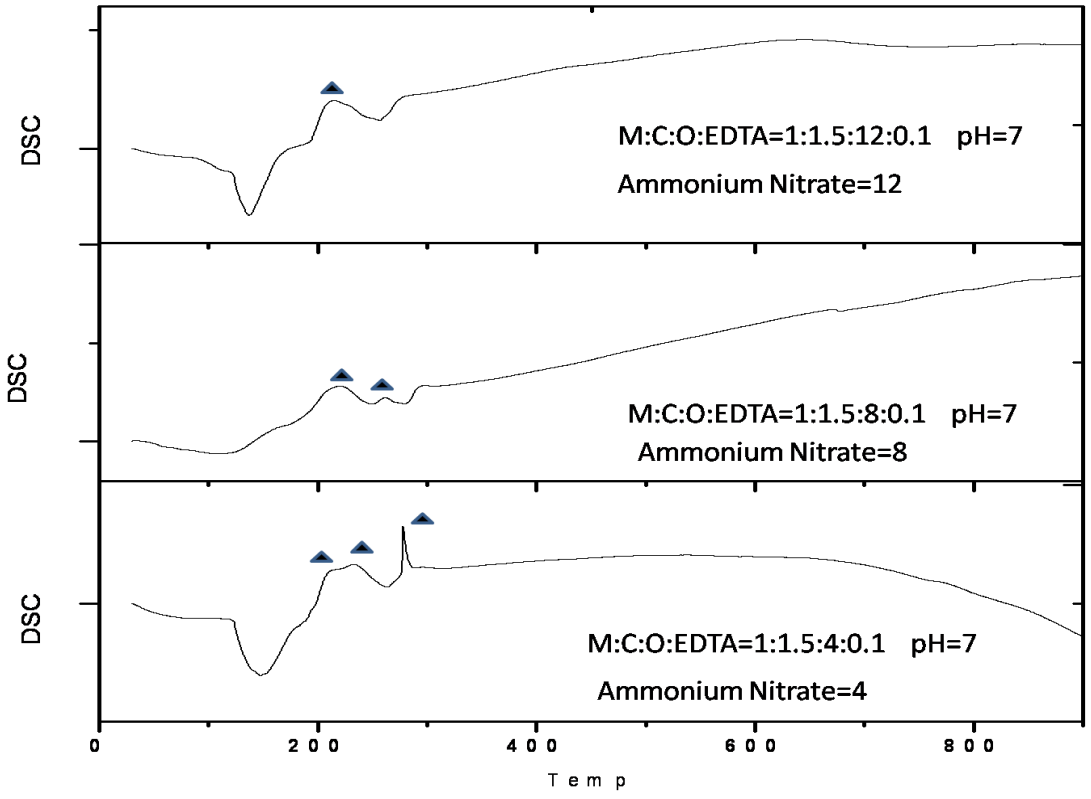

Fig.5.1. DSC pattern of BST precursor gel as a function of ammonium nitrate molar ratio

The DSC pattern of the BST precursor gel showed the existence of three exothermic peaks in the temperature zone 200-300^{o}C when the molar ratio of NH_4NO_3 was 4, while two exothermic peaks was observed in the gel prepared with NH_4NO_3 molar ratio8. It could also be observed that only one exothermic peak in the said temperature zone in the sample prepared with NH_4NO_3molar ratio 12.

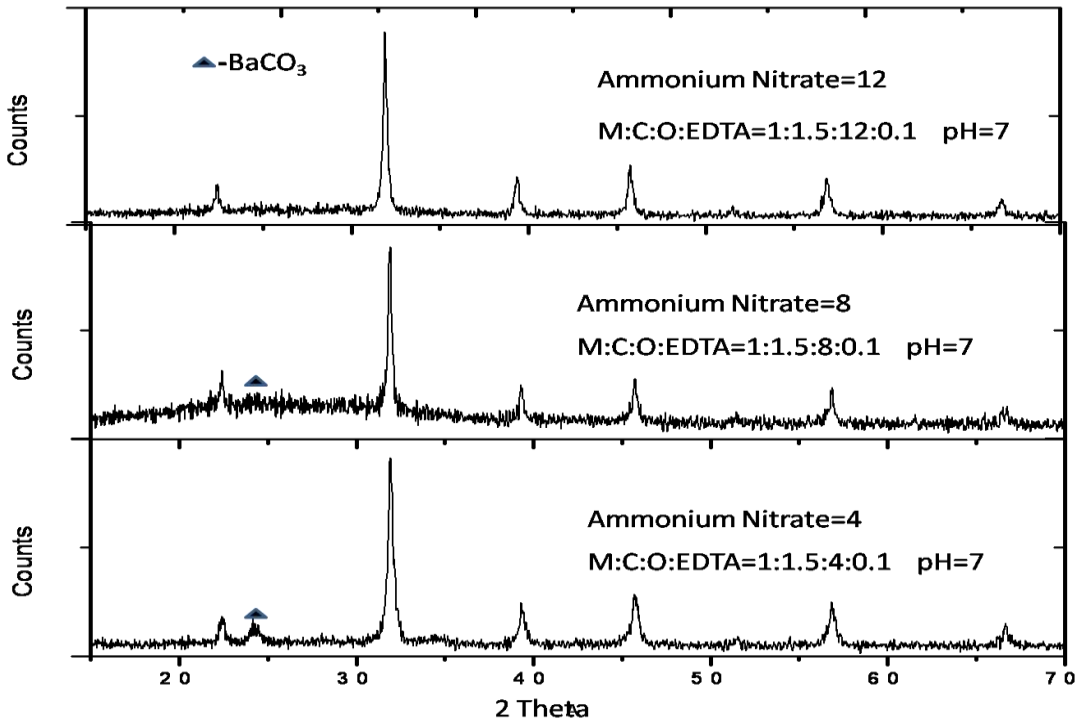

Fig.5.2 XRD pattern of the BST powder as a function of ammonium nitrate in the precursor solution

It could be seen from the figure that trace amount of $BaCO_3$present in the samples prepared with $NH_4NO_3$4 and 8. While it was found that phase pure BST is formed when NH_4NO_3 was 12. No other impurity phases could be detected in the XRD pattern.

Existence of 3 peaks in first case and 2 peaks in second case causes the decomposition of citrate-nitrate complex in 3 and 2 steps respectively, which couldn't yield phase pure powder as a result $BaCO_3$ peaks are observed in the first and second case of the XRD pattern.

5.1.2 Optimization of Citric Acid:

It was confirmed that NH_4NO_3 12 yields a phase pure powder. Hence the CA optimization was studied keeping NH_4NO_3 fixed in molar ration of 12. The molar ratio of CA was varied among, 1, 1.5 and 2.The DSC of the gel as a function of different CA concentration is shown in the Fig. 5.3 and the XRD of the calcined powders calcined at 800°C were shown as a function of different CA concentration is shown in the Fig. 5.4; Table II, shows the different molar ratios in the different batches used for optimizing the CA.

TableII. Molar ratio of different process parameters in different batches for the optimization of CA

Metal(M)	Citric Acid(CA)	NH_4NO_3 (O)	EDTA	pH	Phase Purity
1	1	12	0.1	7	Impure
1	1.5	12	0.1	7	Pure
1	2	12	0.1	7	Impure

The DSC pattern of the BST precursor gel showed the existence of 2 exothermic peaks in the temperature zone 200-300^{o}C when CA was 2, while a single exothermic peak with very low exothermicity was observed in the gel prepared with CA molar ratio1. It could also be observed that only one exothermic peak in the said temperature zone in the sample prepared with CA molar ratio 1.5.

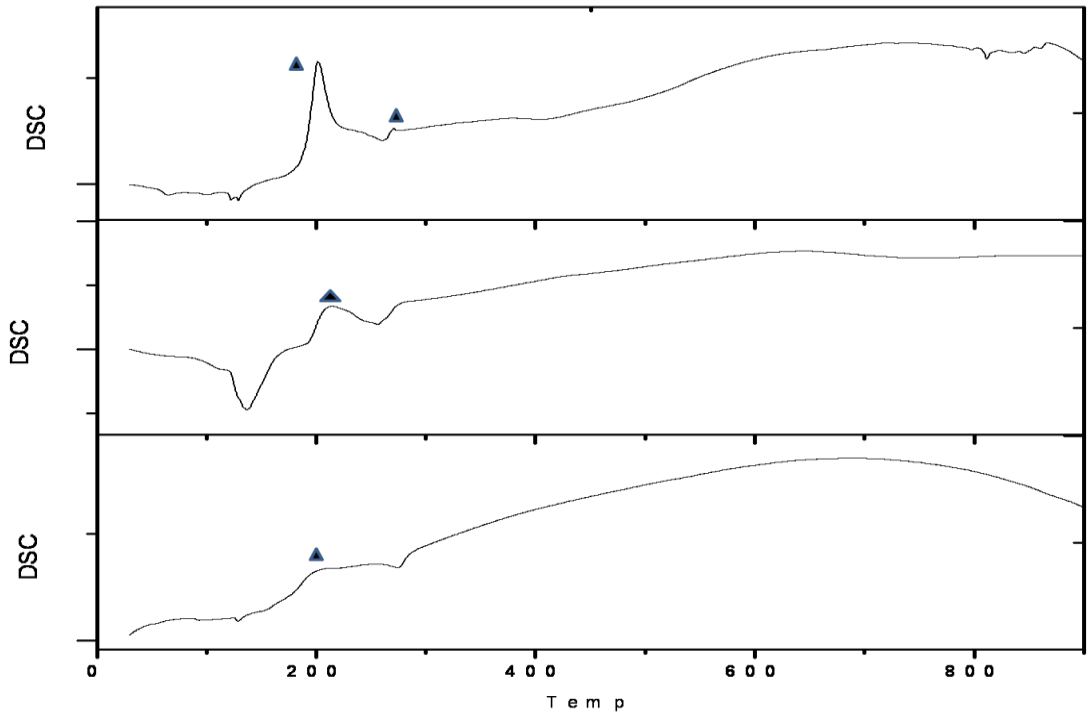

Fig.5.3. DSC pattern of BST precursor gel as a function of citric acid molar ratio

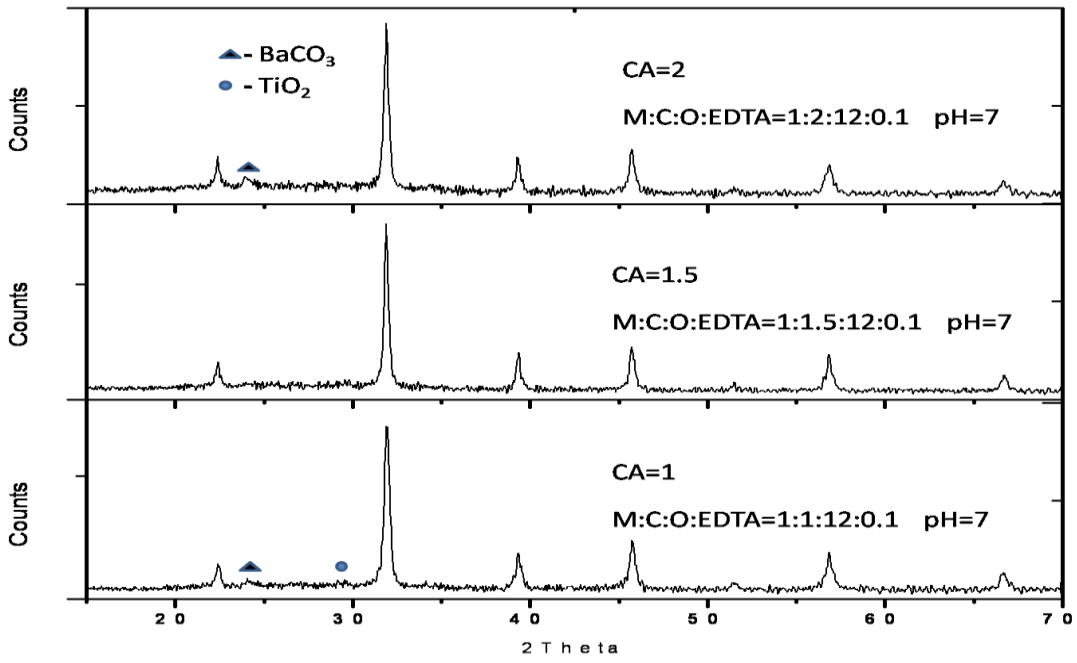

Fig.5.4. XRD pattern of the BST powder as a function of citric acid in the precursor solution

It could be seen from the XRD figure that trace amount of $BaCO_3$present in the samples prepared with CA2 and additional TiO_2, with CA 1. While it was found that phase pure BST is formed when CA was 1.5. No other impurity phases could be detected in the XRD pattern.

Existence of 2 peaks in case of CA 2, first is due to the combustion of the citrate-nitrate complex and the second is due to the combustion of the excess CA present that didn't take part in the chelation, which results in the formation of the impure phase of $BaCO_3$, as the reaction takes place in 2 steps. Impure phase of TiO_2 and $BaCO_3$ is formed with CA 1, due to inadequate chelation.

5.1.3 Optimization of EDTA:

It was confirmed that NH_4NO_3 12 and CA 1.5 yield a phase pure powder. Hence the EDTA optimization was studied keeping NH_4NO_3 and CA fixed in the molar ration of 12 and 1.5 respectively. The molar ratio of EDTA was varied among 0, 0.1 and 0.2.The XRD of the calcined powders calcined at 800°C were shown as a function of different EDTA concentration is shown in the Fig. 5.5; Table III, shows the different molar ratios in the different batches used for optimizing the EDTA.

TableIII. Molar ratio of different process parameters in different batches for the optimization of EDTA

Metal(M)	Citric Acid(CA)	NH_4NO_3 (O)	EDTA	pH	Phase Purity
1	1.5	12	0	7	Impure
1	1.5	12	0.1	7	Pure
1	1.5	12	0.2	7	Impure

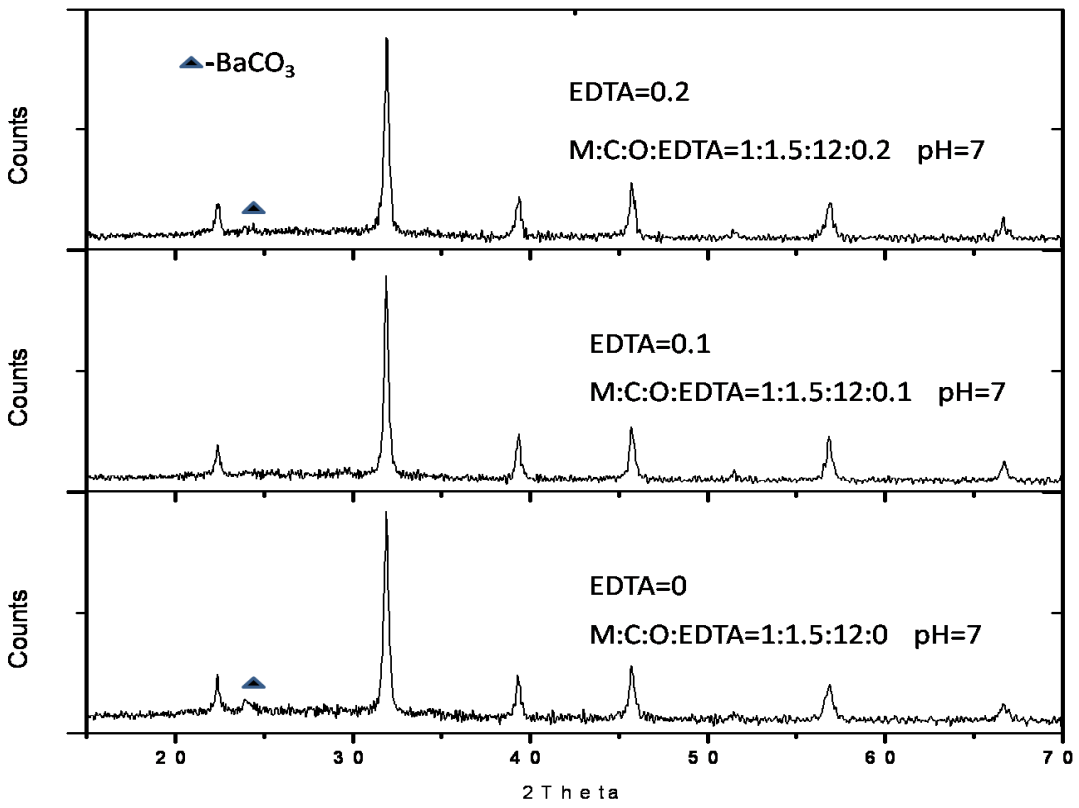

Fig.5.5. XRD pattern of the BST powder as a function of EDTA in the precursor solution

It could be seen from the XRD figure that trace amount of $BaCO_3$present in the samples prepared with EDTA0.2 and 0. While it was found that phase pure BST is formed when EDTA was 0.1. No other impurity phases could be detected in the XRD pattern.

When no EDTA was used, there was incomplete chelation due to which there was some residual $BaCO_3$ phase, and when EDTA was 0.2, there was excess carbon containing species which was responsible for the $BaCO_3$ impure phase.

5.1.4 Optimization of pH:

It was confirmed that NH_4NO_3 12, CA 1.5 and EDTA 0.1 yield a phase pure powder. Hence the pH optimization was studied keeping the above parameters fixed. The pH was varied among 3, 7 and 10.The DSC of the gel as a function of different pH is shown in Fig. 5.6 and the XRD of the calcined powders calcined at 800°C were shown as a function of different pH in the Fig. 5.7; Table IV, shows the different pH in the different batches used for optimizing the CA.

TableIV. Molar ratio of different process parameters in different batches for the optimization of pH

Metal(M)	Citric Acid(CA)	NH_4NO_3 (O)	EDTA	pH	Phase Purity
1	1.5	12	0.1	3	Impure
1	1.5	12	0.1	7	Pure
1	1.5	12	0.1	10	Impure

The DSC pattern of the BST precursor gel showed the existence of 4 exothermic peaks in the temperature zone 200-400^oC when the pH was 3, while two exothermic peaks was observed in the gel prepared with pH in the temperature range 200-300^oC. It could also be observed that only one exothermic peak in the above temperature zone in the sample prepared with pH7. Each peak in DSC corresponds to a single species present in the gel, hence the number of peaks in pH 3 and pH 9, shows that the number of combustible species is more than one.

It could be seen from the XRD figure that trace amount of $BaCO_3$ present in the samples prepared with pH3 and TiO_2, in pH 10. While it was found that phase pure BST is formed when pH was 7 No other impurity phases could be detected in the XRD pattern.

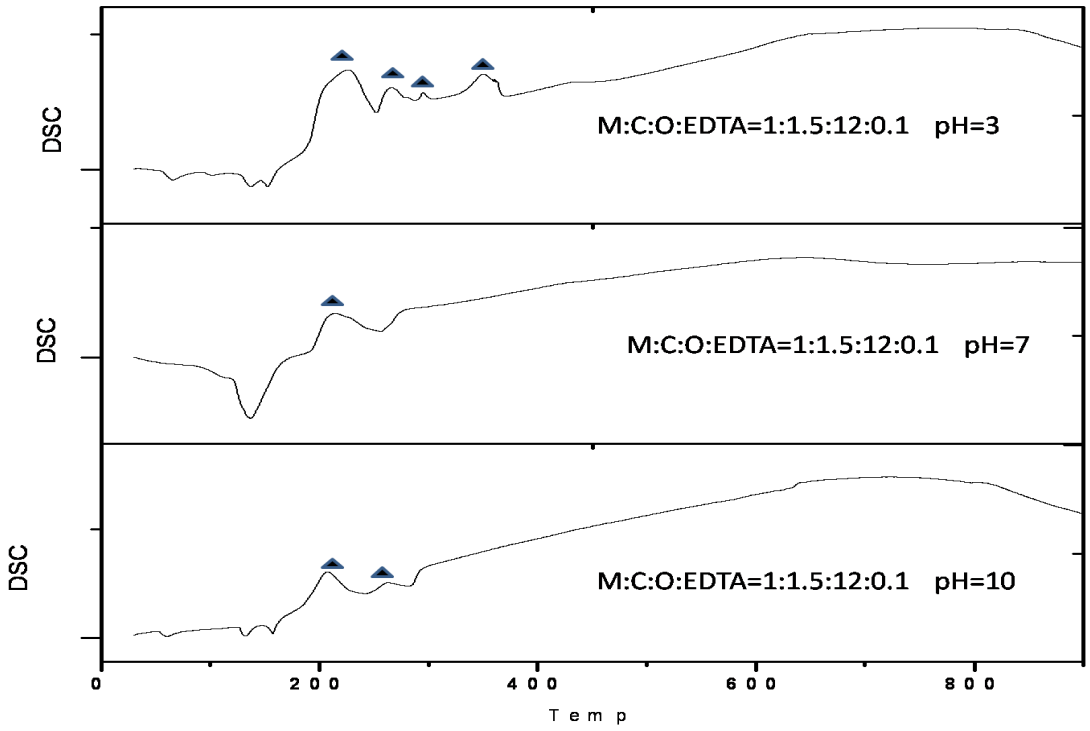

Fig.5.6. DSC pattern of BST precursor gel as a function of pH

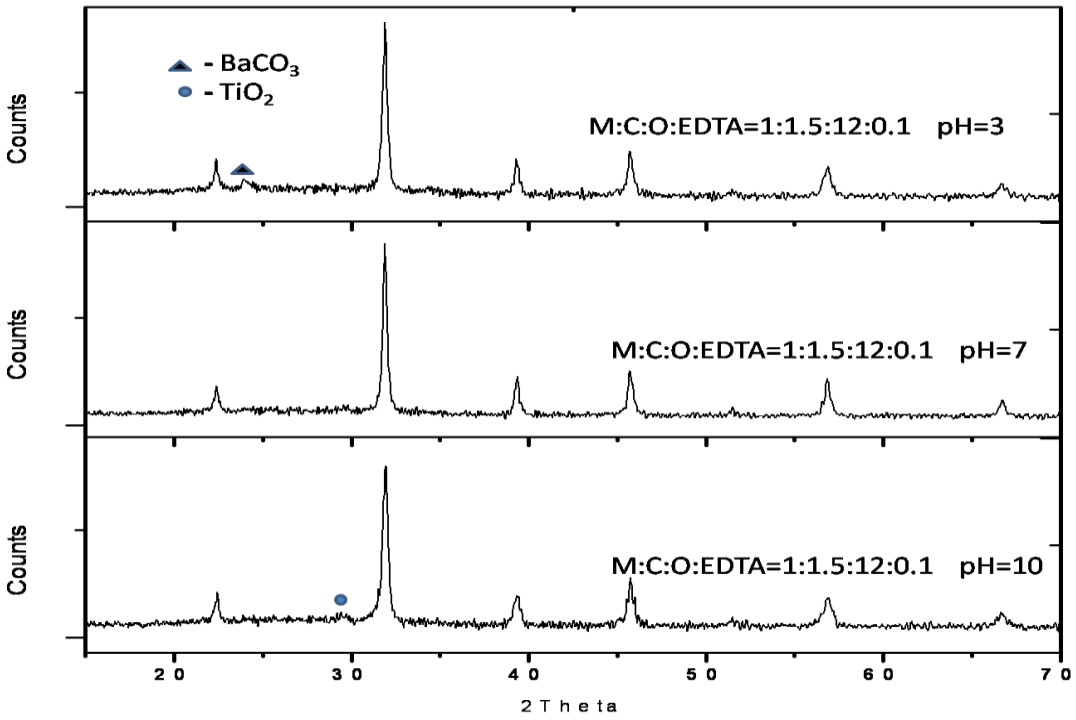

Fig 5.7. XRD pattern of the BST powder as a function of pH

The optimum pH was calculated for synthesizing BST powders by auto-combustion route using citric acid as the chelating agent [9]. It has been reported that Ba^{+2} forms a stable chelation with CA at a pH > 4.58, Sr^{+2} forms a stable chelation with CA at a pH >4.83 and optimum pH at which TiO^{+2} would be chelated with CA is pH < 7. Hence the pH range at which all the above species would be stable is 4.83 < pH < 7. At high pH the CA remains in the form of $HCit^{2-}$ and Cit^{3-}, and the chelating complex of Ba^{+2} and Sr^{+2} with H_2Cit^- wasn't stable hence the pH that was calculated for which the ionic distribution of $H_2Cit^-$was zero was found to be pH < 6.4. From the above data it was calculated that the pH range for the formation of stable BST-CA sol was 6.4<pH<7.

5.2 Synthesis of BST:

Hence BST powders were synthesized from the previously optimized batch of M:CA:NH_4NO_3:EDTA=1:1.5:12:0.1 and at a pH of the precursor solution was 7. All further studies were done at with this optimized batch.

5.2.1 Powder Morphology:

The produced powders were flaky in nature and have a uniform size distribution as evident from its SEM image in Fig. 5.8. The surface area as measured from the BET surface analyzer was found to be4.918 m^2/gm. The particle size was calculated to be 215 nm.

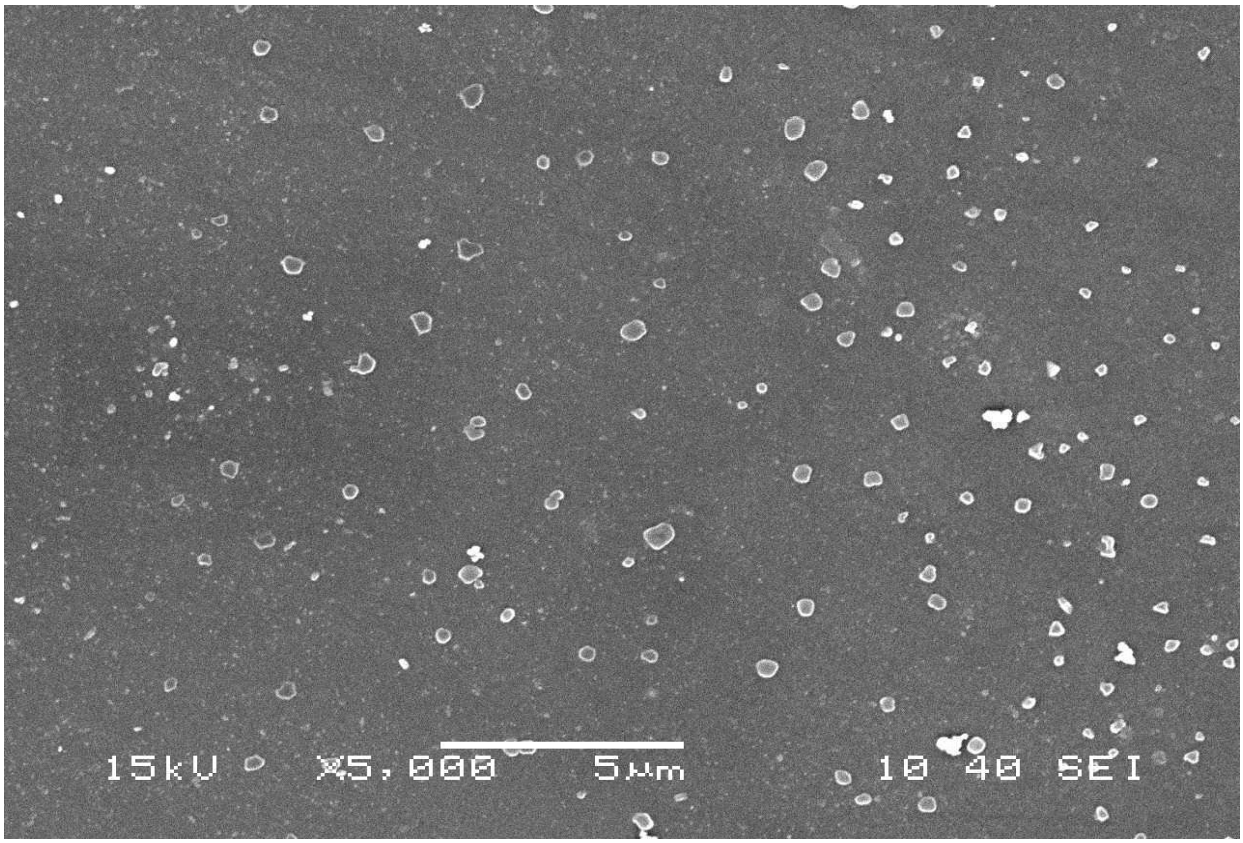

Fig 5.8 SEM image of the BST powder prepared from the optimized batch.

5.3 Sintering Behavior:

Initial stage sintering kinetics has been analyzed for constant rate heating and isothemal heating from the dilatometric data. Attempt has also been made to identify the densification mechanism of BST powder during the initial stage of sintering (assuming solid state densification). It has been well studied that dilatometric data (below 3% shrinkage) could be well fitted with the following equation:

$$T^2\left[\frac{d\,{}^{\Delta L}/_{L}}{dt}\right] = \frac{2Q\beta}{nR}\left[\frac{\Delta L}{L}\right]$$

Where, T is the temperature, $\frac{d^{\Delta L}/_L}{dt}$ is the rate of densification, ΔL is the change in length,Lis the initial length, Q is the activation energy for the sintering, βis the rate of heating, n is the exponent that depends on the mode of sintering and R is the universal gas constant.

So, the plot$\frac{\Delta L}{L}$vs$T^2\left[\frac{d^{\Delta L}/_L}{dt}\right]$, as shown in the Fig.5.9, an approximate straight line is obtained, whose slope would give the value $\frac{2Q\beta}{nR}$ .and from that the value of Q/n was obtained.

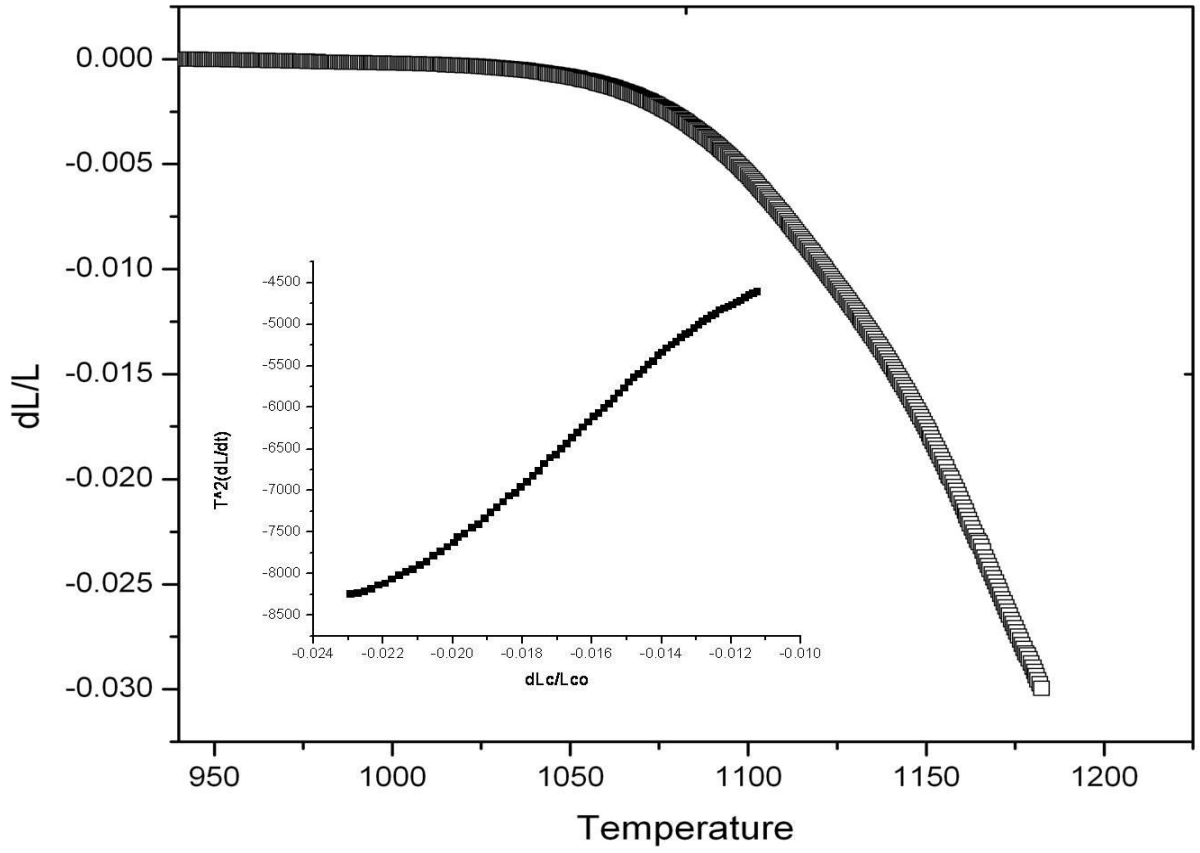

Fig 5.9 Non-Isothermal behavior of the BST powder

The initial stage sintering data for isothermal sintering could be fitted into the logarithmic equivalent of the following equation:

$$\frac{\Delta L}{L} = At^{2/n}$$

Where, ΔL is the change in length, L is the initial length; A is the constant which depends on temperature, t is the time of sintering and n is the exponent that depends on the mode of sintering. The above equation can be written as:

$$\log\frac{\Delta L}{L} = \log A + \frac{2}{n}\log t$$

So the plot of log t vs $\log\frac{\Delta L}{L}$, was shown in Fig.5.10, then the slope of the line would be 2/n, from which the value of n was obtained to be 6.31.

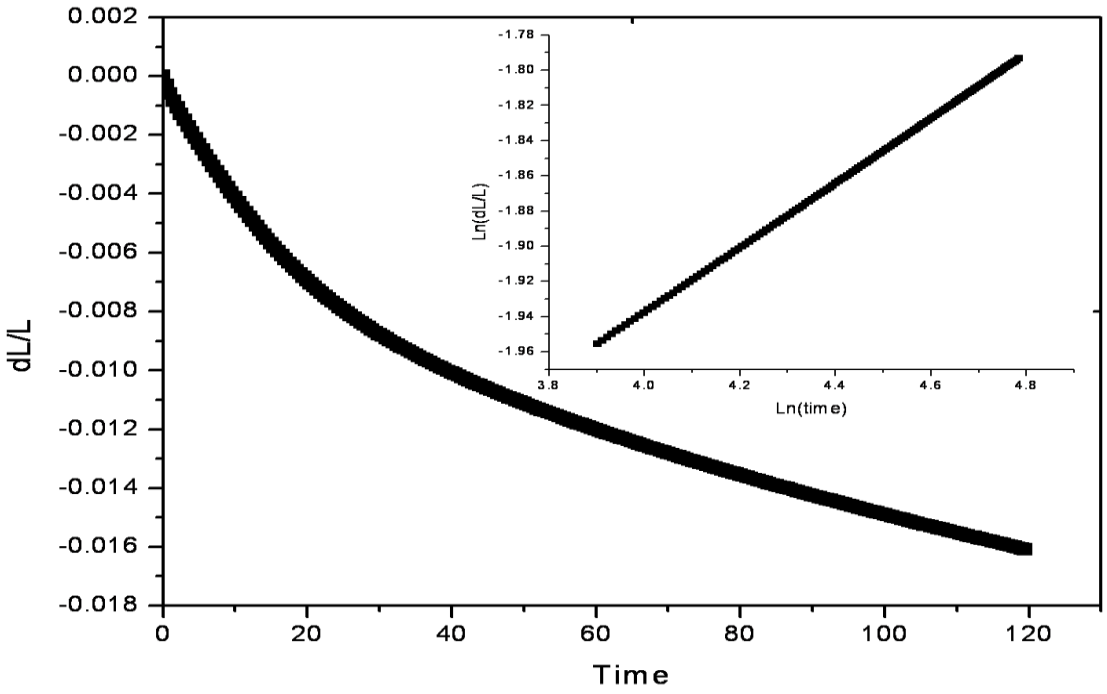

5.10. Isothermal behavior of the BST powder

The value of Q was then calculated by using the value of n. Hence the value of Q was obtained to be around 912 KJ/mol.

5.4Microstructure after Sintering:

The SEM micrographs of the BST samples sintered at 1250°C, 1300°C and 1350°C for 4 hrs have been given in the Fig. 5.11. The average grain has also been provided in the Table V.

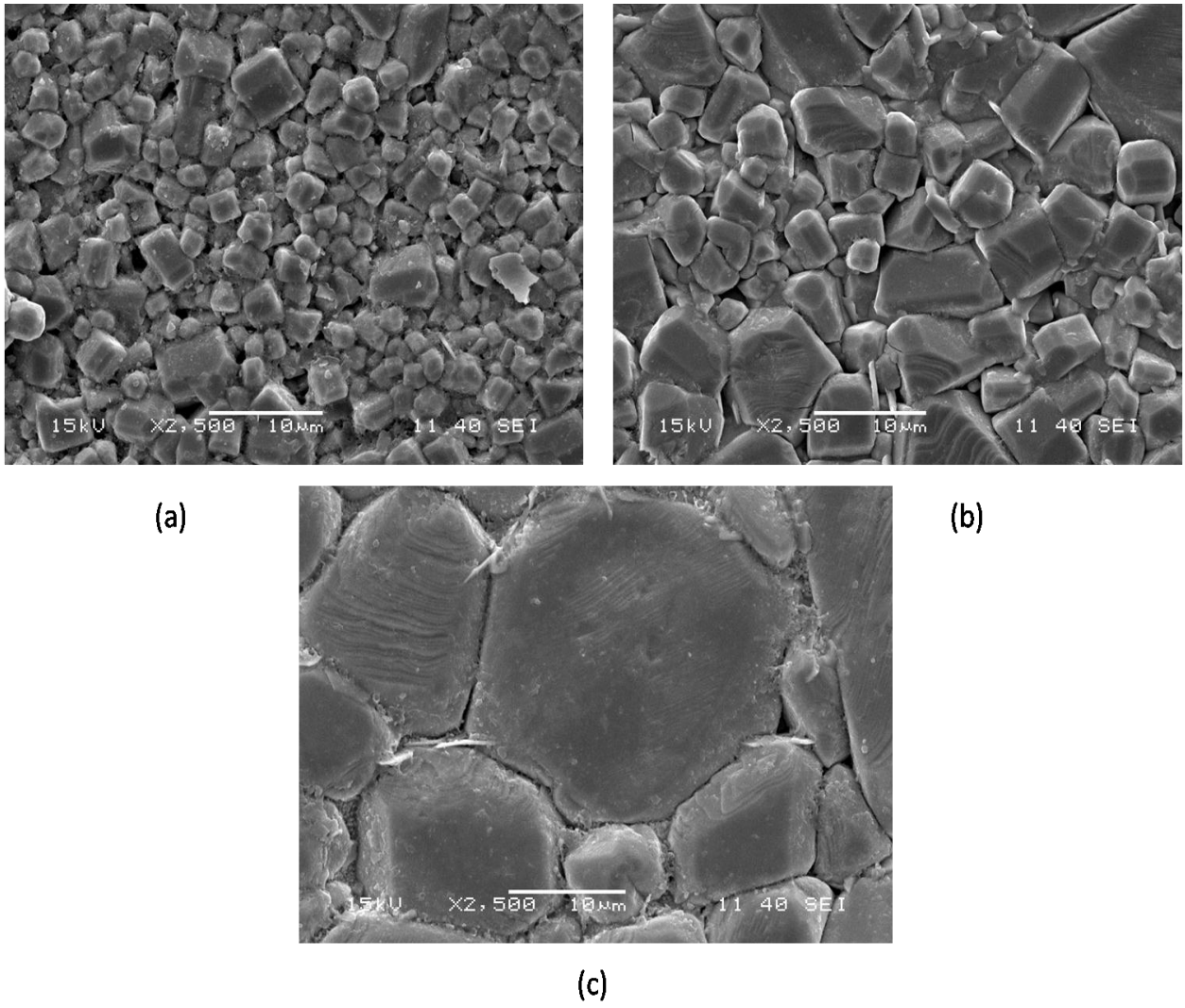

Fig.5.11. SEM micrographs of a. 1250^{o}C/4hrs, b. 1300^{o}C/4hrs, c. 1350^{o}C/4hrs

Table V. Mean Grain size as a function of different sintering temperatures

Temperature	**Size (in micron)**
1250°C/4hrs	2.87
1300°C/4hrs	6.45
1350°C/4hrs	18.25

In 1250^{o}C/4hrs, the image showed almost uniform grain size with a few large grains embedded within the small grain matrix. The large grains are formed due to the agglomerates present in the powder. Porosity is present at the grain boundary only. In 1300^{o}C/4hrs, the image showed obvious effect of grain growth with temperature. Here the smaller grains existed within the matrix of the larger grains. In 1350^{o}C/4hrs, the image showed relatively dense microstructure with large grains present in it. It may be due to the abnormal grain growth of BST ceramics at high temperature.

5.5 Dielectric Behavior of BST:

The frequency dependent as well as temperature dependent dielectric behavior of BST sample sintered at 1350°C/4hrs was studied, as it gave the highest density. The Fig 5.12 shows the results of those studies. Fig 5.12a and Fig 5.12.b shows the relative permittivity (ε_r) and tanδ value of BST as a function of frequency at three different temperatures respectively. The three temperatures are 50°C, 100°C and 150°C. The Fig 5.12c shows the relative permittivity (ε_r) and tanδ value of BST as a function of temperatures at three different frequencies. The three frequencies are 100 KHz, 1 KHz and 100 Hz.

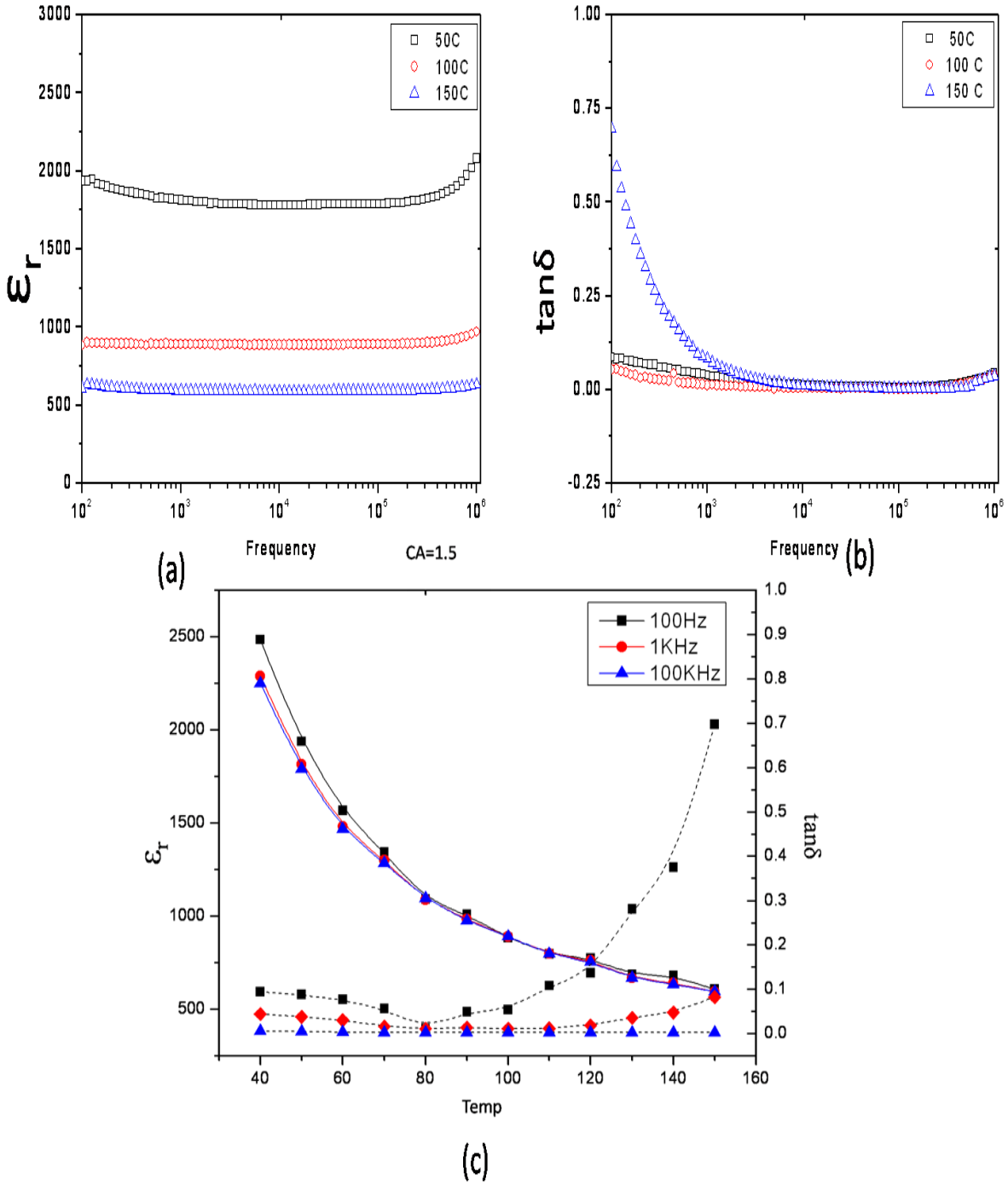

Fig. 5.12. Relative permittivity (a), Loss factor (b) of BST ceramics as a function of frequency at50, 100, 150 Hz, Relative permittivity and Loss factor (c) as a function of temperature at 100Hz, 1KHz and 100KHz

At 50°C the permittivity varies from 2000 to 1800 with respect to frequency, the permittivity has a highest value of around 2400 at 40°C and 100Hz frequency.

The relative permittivity of the BST remained mostly constant for a particular temperature, over the range of frequency. The loss factor tanδ also remained constant for 50°C and 100°C, but for 150°C, it was seen that for low frequency there was high loss but for higher frequencies it became constant. It's because at higher temperature the electronic prolarization in the contact points caused the loss at the lower frequencies. This is the also the reason for the high loss of 100Hz at high temperature.

5.6 Synthesizing BST using Modified Citrate Method:

After the optimization of the citrate-nitrate route, the fuel was changed into 2 different systems; one was a mixture of citric acid and glycine (G)(modified glycine route) and other a mixture of citric acid and ethylene glycol (EG) (modified ethylene glycol route). Different fuel molar ratios were tried and the best ratio was used for the further studies. The other process parameters were kept to the same optimized value as obtained from the previous study. Table VI and Table VII gives the molar ratio of CA:G and CA:EG respectively.

Table VI. Molar ratio combinations of CA and G tried

Citric Acid	Glycine	Phase
1	0.5	Impure
1	1	Pure
1	2	Pure
0.5	1	Impure
0.5	2	Impure

Table VII. Molar ratio combinations of CA and EG tried

Citric Acid	Ethylene glycol	Phase
1	1	Impure
1	2	Pure

As the combustion were done at a pH of 7 and glycine and ethylene glycol at that pH does not act as chelating agent, hence their only job is to help in the combustion process.

For glycine, the molar ratio CA:G of 1:0.5 yield impure phase because the exothermicity may not be high due to the presence of lower amount of fuel, and the last two molar ratio CA:G of 0.5:1 and 0.5:2 gave impure phase either due to improper chelation due to less amount of chelating agent. The molar ratio CA:G of 1:1 and 1:2 gave pure phase, but there was some problem in densification of 1:2 batch maybe due to high particle agglomeration, which is caused due to the presence of excessive fuel amount. For ethylene glycol, only the 2 successful ratios of glycine batch were repeated, and it gave pure phase in only one batch i.e. CA:EG= 1:2.

Hence for further studies the batches that were selected are CA=1.5, and CA:G=1:1 and CA:EG=1:2. The DSC of the gel and XRD pattern of powder as a function of these fuels were shown in the Fig5.13 and Fig5.14 respectively.

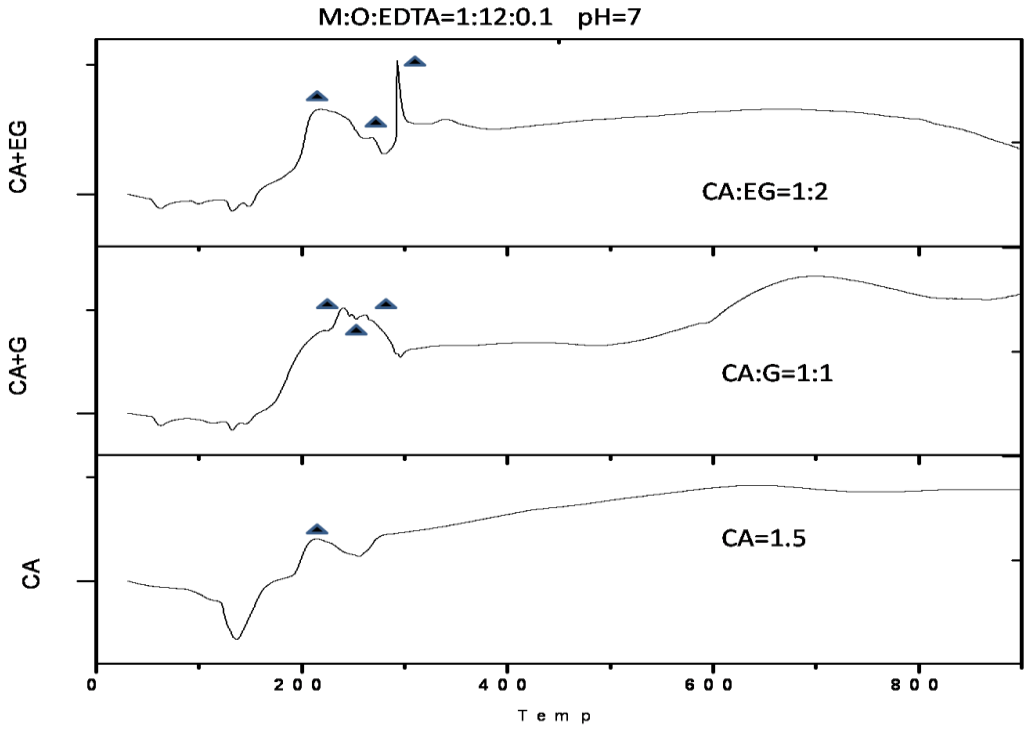

Fig 5.13 DSC of the precursor gel prepared from the three fuel combinations

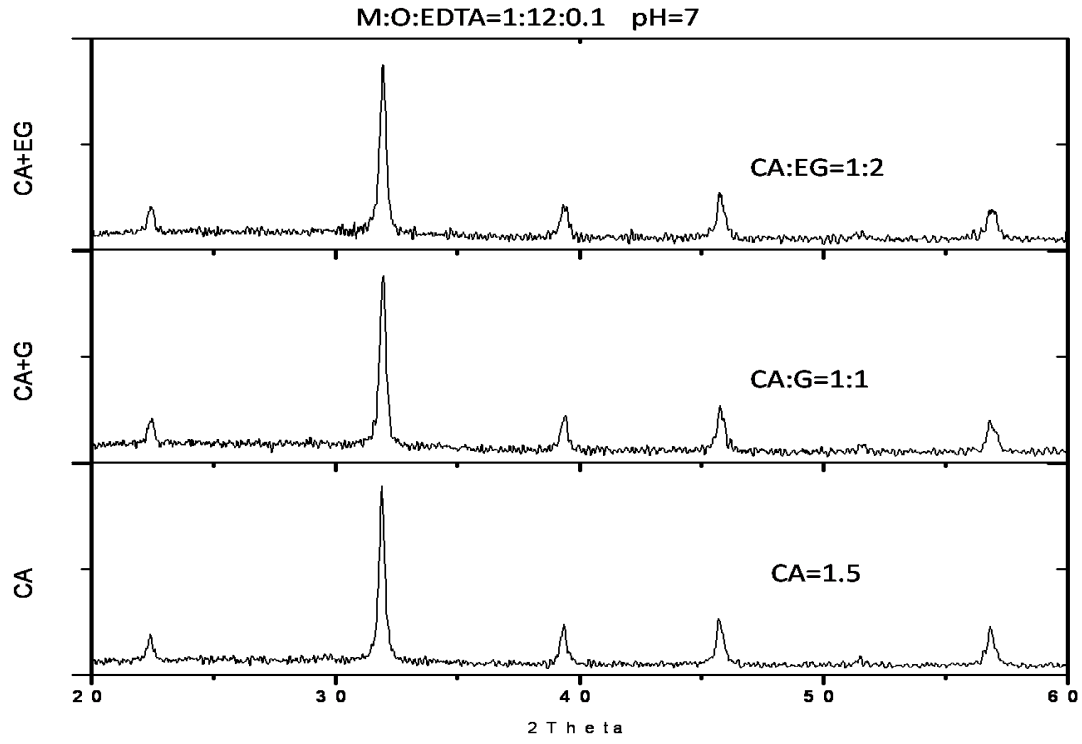

Fig 5.14 XRD of the calcined powder prepared from the three fuel combinations

The DSC plot showed that in case of only CA there is only one single exothermic peak, as explained earlier, in case of CA:G there are about 3 different exothermic peaks and they occur very near to each other which is a convergence of peak found in case of CA and the other would be of combustion of glycine. In case of CA:EG we see the peaks are quite separated to each other and there is no sign of convergence of the CA peak and a sharp exothermic peak which would be due to EG. Analyzing it with the SEM micrographs of the powder sample in Fig 5.15, it can be concluded that the different combustion temperatures may be responsible for the large agglomeration of the powder in case of CA:EG.

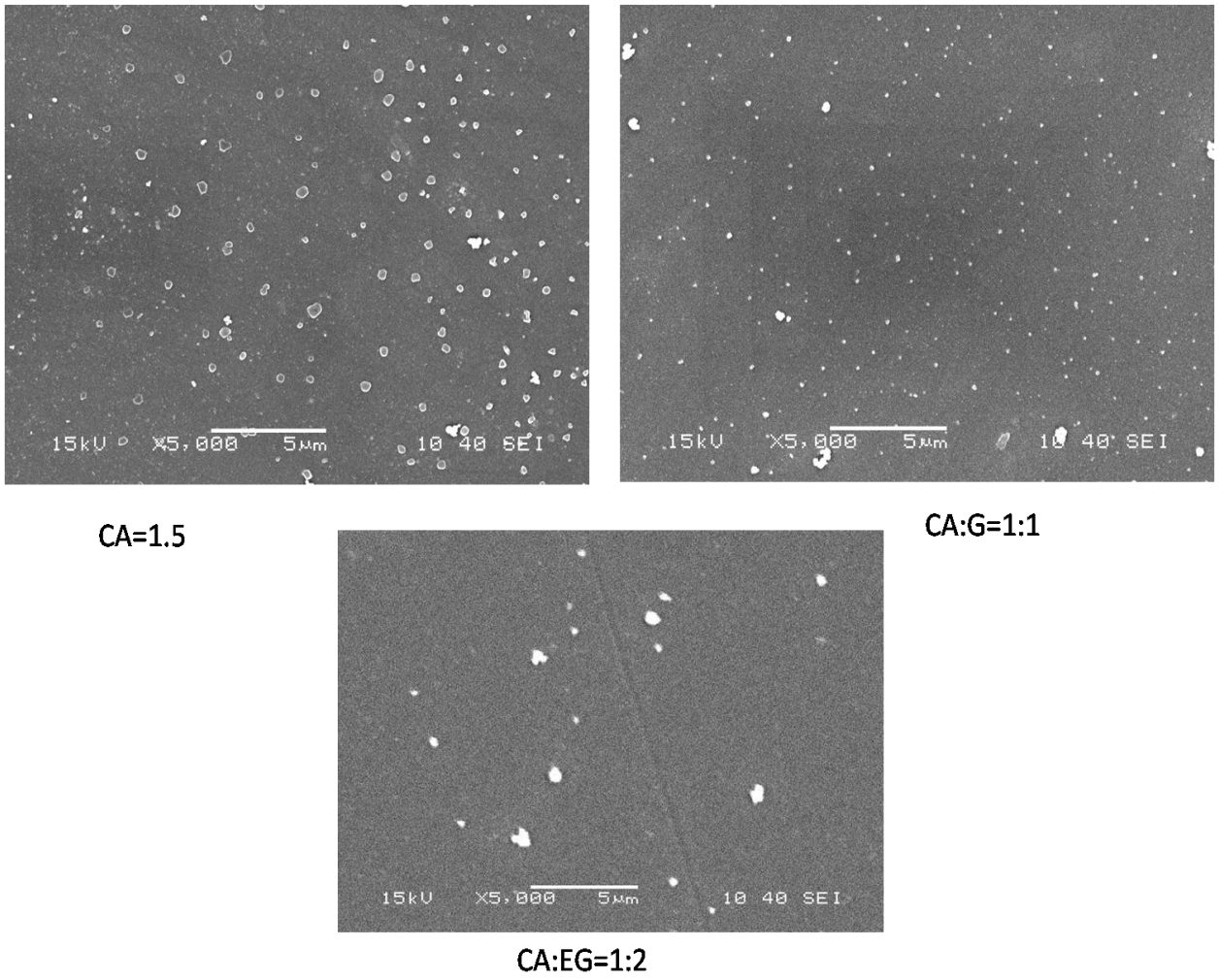

Fig 5.15. SEM micrographs of powders for different fuel combinations

The SEM micrograph showed that the powder in case of CA:G is more uniform and has a lower particle size, and the powder of CA:EG is highly agglomerated in nature.

5.7. Comparative Sintering Behavior:

From the Fig 5.16 and Fig 5.17 it can be clearly seen that in both isothermal and non-isothermal sintering, the batch made with only CA attains a higher densification and that of CA+G and CA+EG, whereas there is nearly same amount of densification in case of CA+G and CA+EG in isothermal case, but CA+EG attains a slightly higher densification than CA+G in non-isothermal sintering.

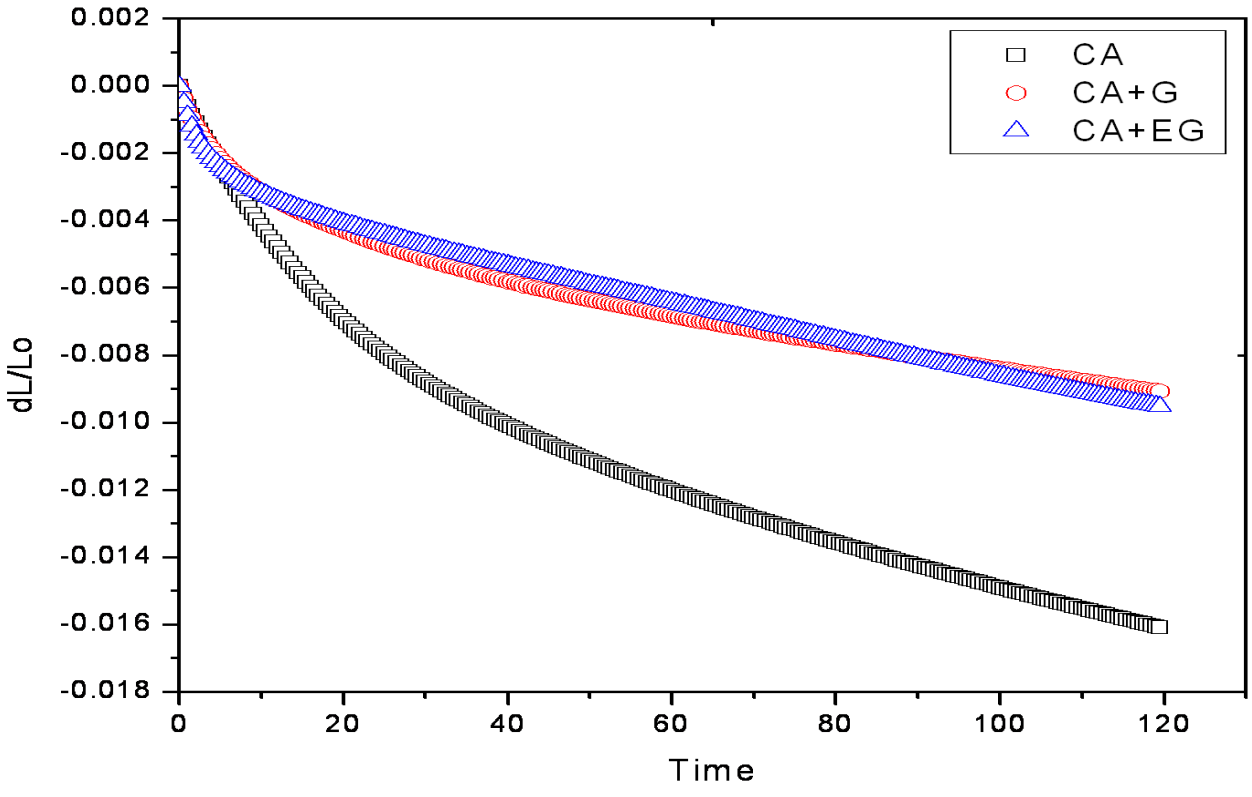

Fig.5.16. Comparative isothermal sintering of BST

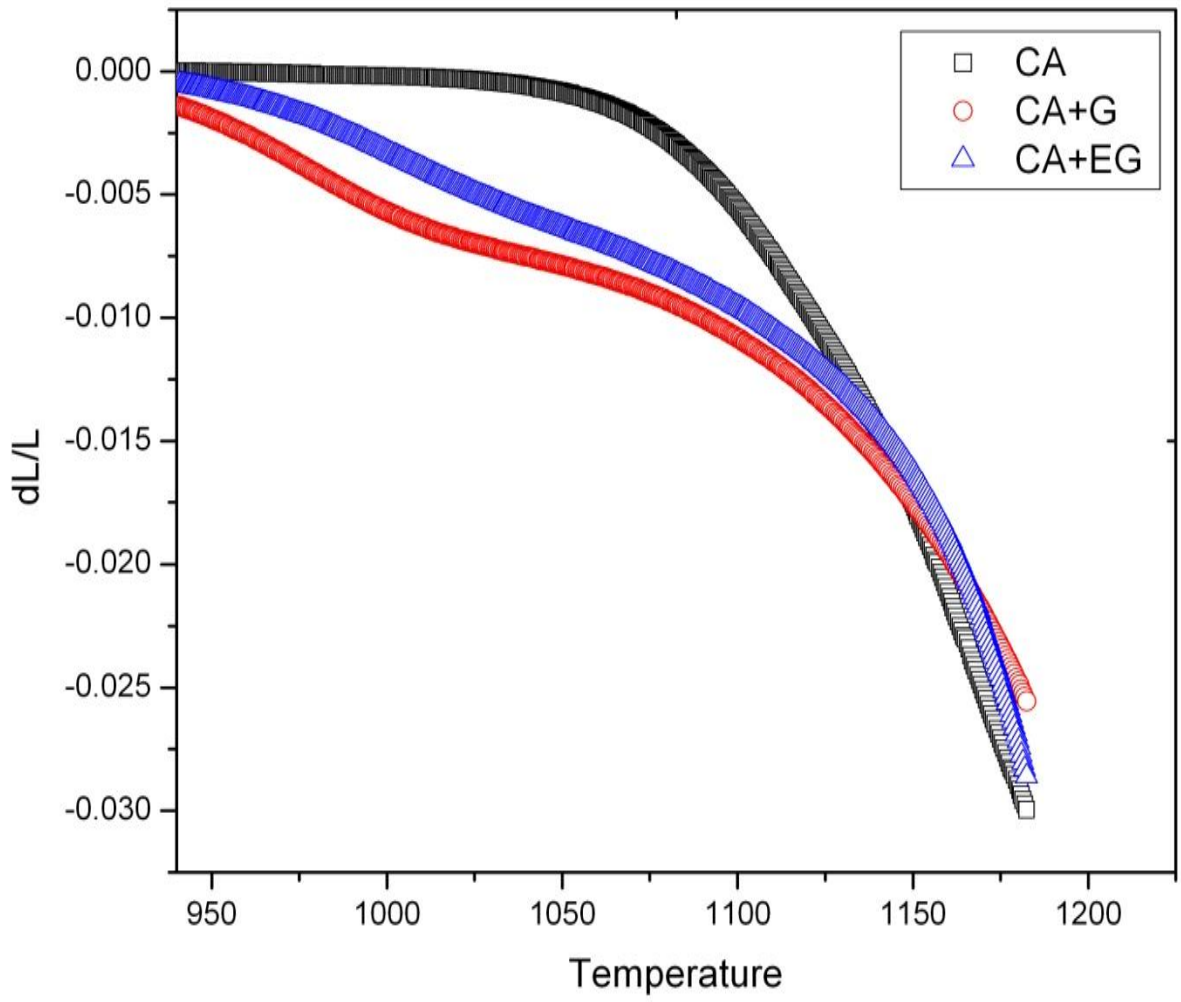

Fig.5.17. Comparative non-isothermal sintering of BST

From the non-isothermal sintering it can be concluded that the sintering of fine powders present in CA+G and CA+EG systems stars to get sinter at a lower temperature than CA system, but their sintering slows down once the sintering of the fine powders are over, while in the meantime the CA batch powders attains densification.

The SEM micrographs of the sintered samples at 1350°C/4hrs are shown in the Fig 5.18.That also matches with the above sintering data.

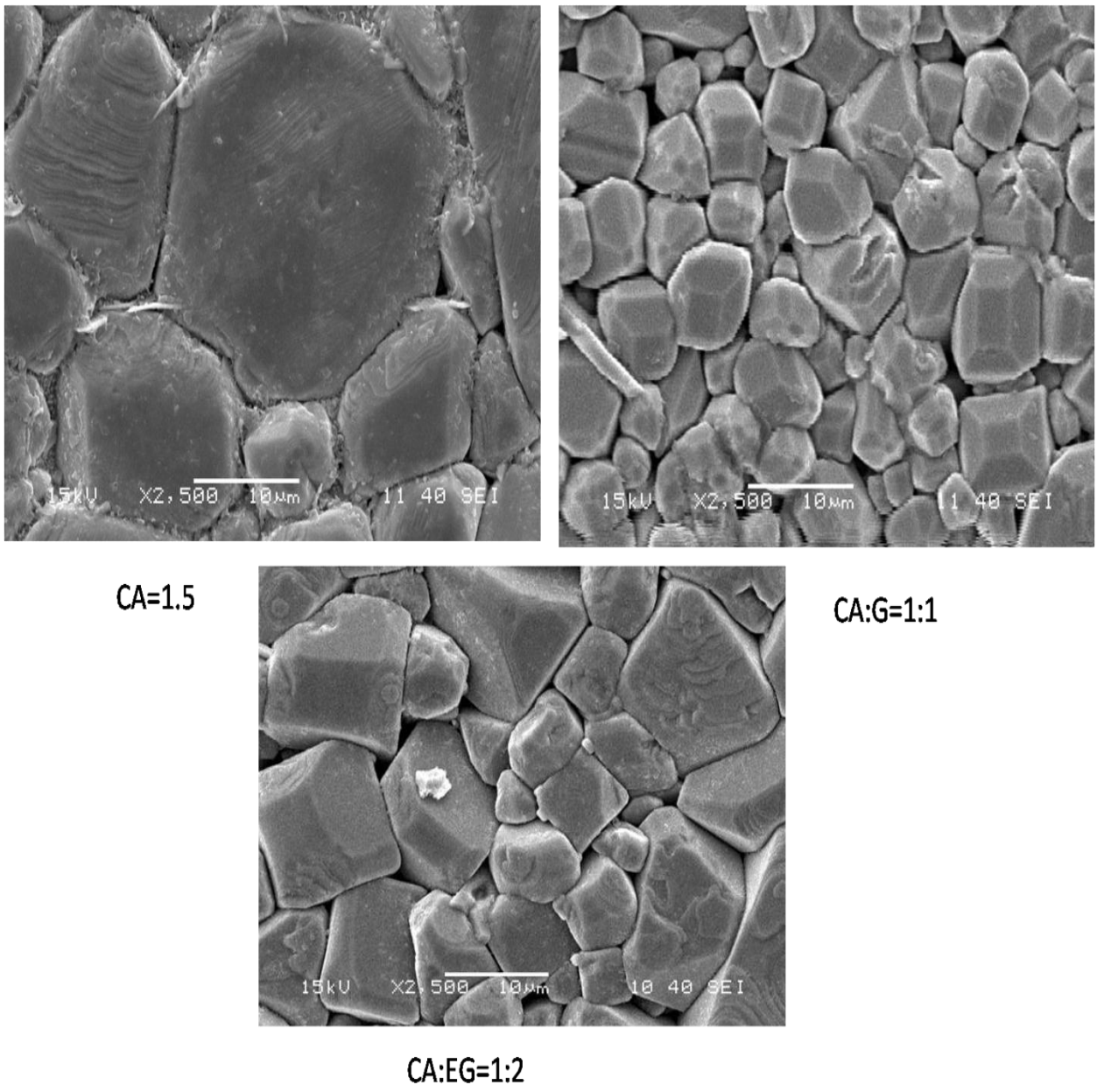

Fig. 5.18. SEM micro graphs of samples sintered at 1350^{o}C/4 hrs

The CA samples have a higher densification and higher grain size. The CA:G sample have some porosity in it, as they are not able to sinter itself to a high density, but still have a more or less uniform grain size distribution. The CA:EG samples have some porosity in it as its not able to sinter to a higher density, and it has a very non-uniform and highly disordered grain size. The average grain size of the above samples is given in the Table VIII.

Table VIII. Mean Grain size as a function of fuel systems

Fuel	Size(in micron)
CA	18.25
CA+G	6.80
CA+EG	13.50

5.8. Comparative Dielectric Behavior:

The dielectric behavior of different samples sintered at 1350°C/4hrs, was studied, and the results were plotted in Fig5.19 as a function of different fuels. The dielectric permittivity and the loss factor were plotted against temperature for three different frequencies (100Hz, 1 KHz and 100 KHz).

In all the cases the CA samples gave much higher dielectric permittivity and low loss, its mainly because of the fact that they have been sintered to a higher density. The CA+G and CA+EG samples though have nearly equal amount of porosity, still the former is giving much higher dielectric permittivity and the low loss due to its small grain size.

The gap between the dielectric permittivity of different samples at a particular frequency increases with increasing the frequency. It is due to the ionization of the air gaps present in the porous samples

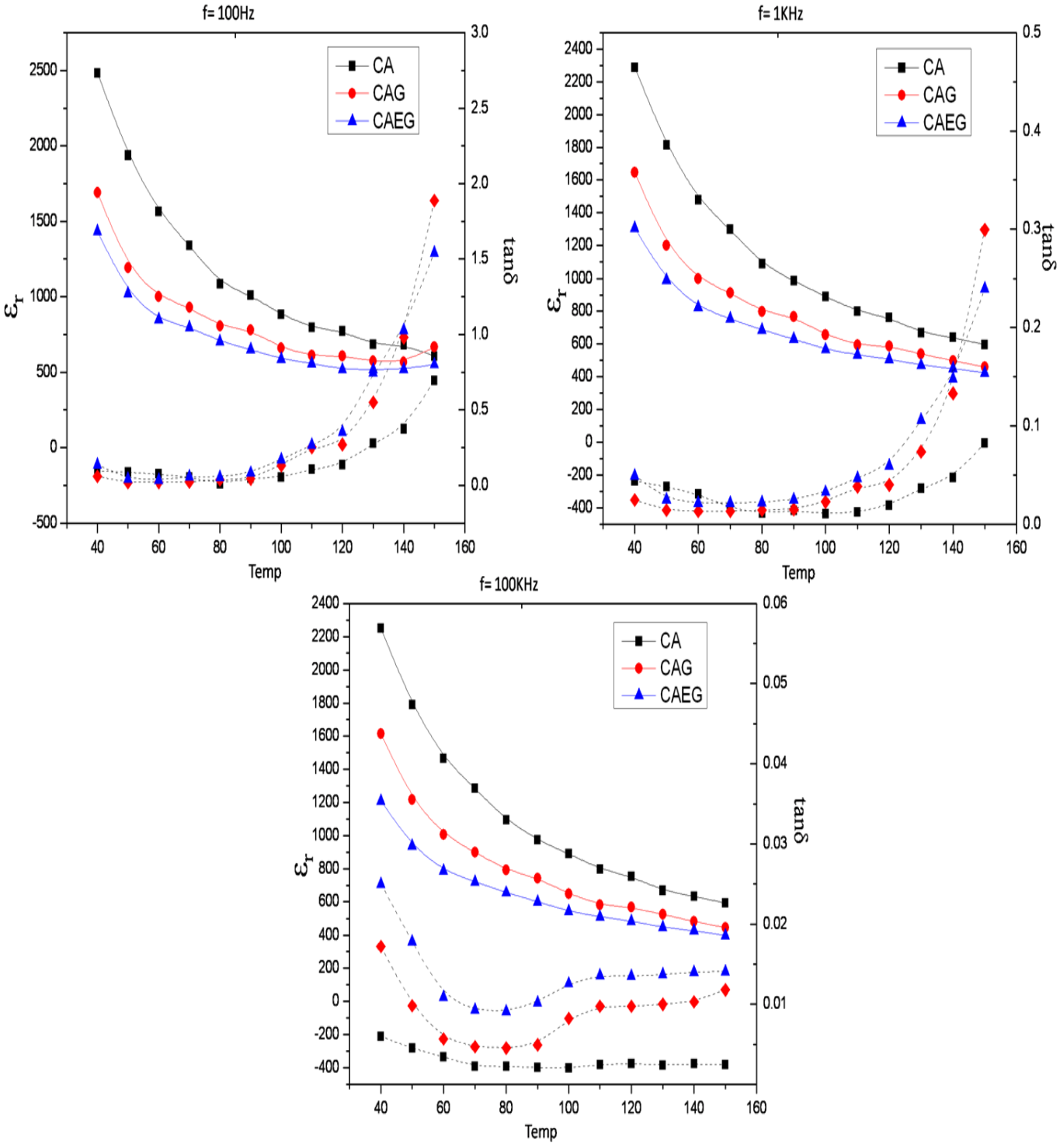

Fig. 5.19. Comparative Dielectric Behavior of different fuel systems as a function of different frequencies.

Chapter 6

Conclusion and Scope of Further Work

6.1 Conclusion

Optimized process parameters for citrate-nitrate combustion synthesis were found to be Metal: Citric Acid: Ammonium Nitrate: EDTA is: 1:1.5:12:0.1 at pH of the precursor solution was 7. The studies with different fuel ratio showed that CA:G produced best results when used in a molar ration of 1:1 and CA:EG produced best results when mixed in a ratio of 1:2, with the other optimized process parameters of the citrate-nitrate combustion synthesis. Among these the best result is shown when only Citric Acid is used, but the CA+G fuel produced a more uniform particle size distribution.

The fuel mixture of CA+G gives better dielectric property than CA+EG because the former had a more uniform and small grain size distribution than the later. Dielectric properties have a direct relation on porosity, grain size, and grain size distribution.

6.2 Scope of Further Work:

- Optimization of modified glycine route can be studied so as to produce a more uniform and narrow grain size distribution with high densification
- More work needed to be done on the Citric Acid route so as to optimize the different parameters by changing more than one parameter simultaneously.
- Dielectric behavior of optimized CA samples can be studied as a function of sintering temperature and sintering schedule.

References

References:

1. C. Mao, X. Dong, T. Zeng, H. Chen and F. Cao, "Nonhydrolytic sol–gel synthesis and dielectric properties of ultrafine-grained and homogenized $Ba_{0.70}Sr_{0.30}TiO_3$",Ceramics International 34 (2008), 45-49
2. F. Zimmermann, M. Voigts, W. Menesklou and E. Ivers-Tiffée, "$Ba_{0.6}Sr_{0.4}TiO_3$ and $BaZr_{0.3}Ti_{0.7}O_3$ thick films as tunable microwave dielectrics", Journal of the European Ceramic Society 24 (2004), 1729-1733
3. T. Bonaedya, K.M. Songa, K.D. Sunga, N. Hura and J.H. Jung, "Magnetoelectric and magnetodielectric properties of $(1-x)Ba_{0.6}Sr_{0.4}TiO_3$–$(x)La_{0.7}Ca_{0.3}MnO_3$ composites", Solid State Communications 148 (2008), 424-427
4. S Wanga, J Zhai, X Choua, L Zhanga and X Yaoa, "Dielectric tunable properties of $Ba_{0.6}Sr_{0.4}TiO_3$–$BaZn_6Ti_6O_{19}$ microwave composite ceramics", Materials Chemistry and Physics 115 (2009), 200-203
5. Q Xua, X Zhanga, H Liua, W Chena, M Chenb, B Kimb, "Effect of sintering temperature on dielectric properties of $Ba_{0.6}Sr_{0.4}TiO_3$–MgO composite ceramics prepared from fine constituent powders", Materials & Design 32(2011), 1200-1204
6. T. Wang, F. Gaoa, G.Hua and C.Tiana,"Synthesis $Ba_{0.6}Sr_{0.4}TiO_3$–$ZnNb_2O_6$ composite ceramics using chemical coating method", Journal of Alloys and Compounds 504 (2010) 362-366.
7. H Megaw, "Changes in Polycrystalline Barium-Strontium Titanate at its Transition Temperature", Nature 157(1946), 20-21
8. M.R Mohammadi, D.J. Fray, "Sol–gel derived nanocrystalline and mesoporous barium strontium titanate prepared at room temperature", Particuology, (in Press) (2011),

http://www.sciencedirect.com/science?_ob=ArticleURL&_udi=B8JJD-52FCTXN-2&_user=1657113&_coverDate=03%2F22%2F2011&_rdoc=1&_fmt=high&_orig=gateway&_origin=gateway&_sort=d&_docanchor=&view=c&_acct=C000053917&_version=1&_urlVersion=0&_userid=1657113&md5=fadfd00da93c1dbca94fbd6453f7d1de&searchtype=a

9. D Dong, X Liu, H Yu, W Hu, " Fabrication of highly dispersed crystallized nanoparticles of barium strontium titanate in the presence of N,N-dimethylacetamide",Ceramics International 37 (2011), 579-583
10. Y.B. Khollam, S.B. Deshpande, H.S. Potdar, S.V. Bhoraskar, S.R. Sainkar, S.K. Date, "Simple oxalate precursor route for the preparation of barium–strontium titanate: $Ba_{1-x}Sr_xTiO_3$ powders", Materials Characterization 54 (2005), 63-74
11. M Li, M Xu, "Preparation of cauliflower-like shaped BST powders by modified oxalateco-precipitation method", Journal of Alloys and Compounds 474 (2009), 311-315
12. S.H. Xiao, J Hu, H.J Xu, W.F Jiang, X.J Li, "The calculation of the optimum pH range for synthesizing BST nano powders by sol-gel auto-combustion process", Journal of Sol-Gel Science and Technology 49 (2009), 166-169
13. X.H Zuo, X.Y Deng, Y Chen, M Ruan, W Li, B Liu, Y Qu, B Xu, "A novel method for preparation of barium strontium titanatenanopowders", Materials Letters 64 (2010), 1150-1153
14. C Shen, Q Liu, Q Liu, "Sol–gel synthesis and spark plasma sintering of $Ba_{0.5}Sr_{0.5}TiO_3$", Materials Letters 58(2004), 2302-2305
15. Y Xiaowei, Z Yanwei, M Leiqing, H Longxiang, "Oleic acid assisted glycothermal synthesis of cuboidal $Ba_{0.6}Sr_{0.4}TiO_3$nanocrystals and their ordered architectures via self-assembly", Journal of Colloid and Interface Science 357 (2011), 308-316

16. X.H Zuo, X.Y Deng, Y Chen, M Ruan, W Li, B Liu, Y Qu, B Xu, “A novel method for preparation of barium strontium titanatenanopowders”, Materials Letters 64 (2010), 1150-1153
17. Y Xiaowei, Z Yanwei, M Leiqing, H Longxiang, “Rapid synthesis of quasi-spherical (Ba,Sr)TiO_3nanocrystals via a microwave-activated glycothermal approach”, Journal of Materials Chemistry 21 (2011), 3133-3141
18. B Hou, Y Xu, D Wu, Y Sun, “Preparation and characterization of single-crystalline barium strontium titanatenanocubes via solvothermal method”, Powder Technology 170(2006), 26-30
19. J.Q Qi, Y Wang, W.P Chen, L.T Li, H.L.W Chan, “Direct large-scale synthesis of perovskite barium strontium titanatenano-particles from solutions”, Journal of Solid State Chemistry 178 (2005), 279-284
20. S Maensiri, W Nuansing, J Klinkaewnarong, P Laokul, J Khemprasit, “Nanofibers of barium strontium titanate (BST) by sol–gel processing and electrospinning”, Journal of Colloid and Interface Science 297(2006), 578-583
21. C Berbecaru, “Synthesis and dielectric characterization of $Ba_{0.6}Sr_{0.4}TiO_3$ ferroelectric ceramics”, Thin Solid Films Article in Press(2011), http://www.scopus.com/record/display.url?eid=2-s2.0 78651354104&origin =resultslist &sort=plff&src=s&st1=Berbecaru&sid=MpO2vtd2p35qMB2voeYYC5R%3a30&sot=b&sdt=b&sl=22&s=AUTHORNAME%28Berbecaru%29&relpos=2&relpos=2&searchTerm=AUTHOR-NAME(Berbecaru)
22. A.Z Simões, F Moura, T.B Onofre, M.A Ramirez, J.A Varela, E Longo, “Microwave-hydrothermal synthesis of barium strontium titanate nanoparticles”, Journal of Alloys and Compounds 508 (2010), 620-624

23. S Lahiry, A. Mansingh, “Dielectric properties of sol–gel derived barium strontium titanate thin films”, Thin Solid Films 516 (2008), 1656-1662